Levelised cost of energy analysis for offshore wind farms – A case study of the New York State development

Yibo Liang[a], Yu Ma[b], Haibin Wang[a], Ana Mesbahi[a], Byongug Jeong[a], Peilin Zhou[a,c,1]

[a] *Department of Naval Architecture, Ocean and Marine Engineering, University of Strathclyde, Glasgow, G4 0LZ, UK*

[b] *Department of Mechanical Engineering, Massachusetts Institute of Technology, Cambridge, MA 02139, USA*

[c] *Ocean Engineering Faculty, Zhejiang University, Zhoushan, 316021, China*

Abstract

In the present work, a comprehensive numerical model was developed to predict the levelised cost of energy (LCOE) for offshore wind farms. A case study is further performed based on the potential developments at the offshore area of the New York State. In the present work, some specific local limitations in the United States are considered by following in line with the present European development experience. A ten-year historical wind data set is used to evaluate the wind farm energy production. The effects of distance to shore, rated power, life span, operation height, farm capacity and seasonal operation plan on LCOE are evaluated. An optimal site giving an LCOE of 123.4 $\$^{2018}$/MWh is found in this paper. In addition, a novel factor named as wind farm energy density (WFED) is suggested in the present study. It shows that when considering the limited coastal area as an issue, a large capacity wind farm may not have good performance compared with a lower capacity wind farm in terms of energy production. The 508 MW wind farm has a better WFED compared with either a 330 MW wind farm or an 800 MW wind farm under the current investigation.

Keywords

Levelised cost of energy (LCOE); Offshore wind farm; Life cycle analysis (LCA)

Nomenclature

[1] Corresponding author e-mail address: peilin.zhou@strath.ac.uk

C	Future amount of money at time t
C_3	3 MW turbine installation cost function
C_6	6 MW turbine installation cost function
C_{10}	10 MW turbine installation cost function
C_{ps}	Port and staging cost
C_s	Turbine installation cost
C_t	Substructure installation cost
CAPEX	Capital expenditure
D_p	Distance from port to project site
DF	Debt fraction
E	Transformer voltage
E_t	Energy generated
HVDC	High Voltage Direct Current
I	Grid current
I_t	Investment expense
i	Inflation rate
IR	Interest rate
l	Cable length
LCA	Life cycle analysis
LCCA	Life cycle cost analysis
LCOE	Levelised cost of energy
M_t	Operation and maintenance costs
O & M	Operation and maintenance
OPEX	Operating expenditure

P	Active power of the turbine
P_{loss}	Ohmic power losses
PDF	Power density function
PPI	(Industrial) Producer Price Index
PV	Present value
R	Cable resistance
r	Discount rate
$RROE$	Rate of return on equity
t	Time
$TaxRate$	Tax rate combined state and federal tax rate
TR	Turbine rating in megawatts
W_d	Maximum water depth at project site
$WACC$	Weighted Average Cost of Capital
x_c	Interpolated installation cost
$\$^{2018}$	U.S. dollars in January 2018
$£^{2016}$	Pound sterling in January 2016
$€^{2012}$	Euro in January 2012

1. Introduction

1.1. Overview of offshore wind energy

More than 100 countries have agreed to keep a global temperature rise this century well below 2 degrees Celsius (Meinshausen et al., 2009). Therefore, offshore wind energy has attracted strong attention around the world. Since 2004, the sector of offshore wind development has had a sustained and rapid annual growth, the European offshore wind power grew from 0.3 Mtoe (million tonnes of oil equivalent) to 2.8 Mtoe in 2014 and is expected to reach at 11.7 Mtoe in 2020 according to the report published by the European Environment Agency (EEA, 2017). Among the developments within the offshore wind sector, UK offshore wind acts as a frontrunner, where over 20.8 TWh in 2017 has been generated supplying 6.2% of the UK's total estimated electricity generation (The Crown Estate, 2017) which reduced the UK's CO_2 emissions by 8.6 million tonnes. Apart from the European countries, the United States offshore wind energy has a technical resource potential of more than 2,000 GW of capacity, equivalent to 7,200 TWh of electricity generation per year (Hartman, 2016). After a decade of developing the offshore wind industry, the United States offshore wind community shows a positive trend. In order to develop the capacity of the offshore wind sector, the state of New York has set a target to developing 2,400 MW of capacity on offshore wind by 2030 (Authority, 2017). There are numerous advantages for utilising offshore wind energy when it is compared with the onshore wind farm, such as higher wind speed, greater applicable areas and more convenient transportation during installation/operation. However, there are still some challenges for offshore wind development when considering a long life span (20 – 30 years). For example, the high capital expenditure (CAPEX) and operating expenditure (OPEX) significantly limit the utilisation of offshore wind energy. Thus, at the moment, detailed studies on CAPEX and OPEX are still in high demand and are often used for initial review of the offshore wind farm investment.

1.2. Previous developments on levelised cost of energy (LCOE)

While determining their energy management policies, it is of paramount importance for coastal states to have a clear understanding on the relative cost-effectiveness and feasibility of offshore wind energy technologies. The levelised cost of energy (LCOE) methodology models every aspect of the reality to create a benchmarking or ranking tool to evaluate the cost-effectiveness of different energy generation technologies or plans (Branker et al., 2011; Hegedus and Luque, 2010; Short et al., 1995). The LCOE analysis evaluates results from the life cycle cost assessment with regards to measuring lifetime costs divided by energy production. Reporting the erroneous LCOE values of technologies can result in not only sub-optimal decisions for a specific project, but can also misguide policy initiatives at the local and global scale, especially for offshore wind energy. To date, there is still a lack of understanding on the assumption and justification of the LCOE values for most of the renewable energy technologies. A good understanding and determination of the LCOE values will serve as a benchmark for decision making and policy initiative. Among different renewable energy technologies, there is a relatively good understanding of the LCOE values on solar photovoltaic technology. A comprehensive review of the solar photovoltaic levelised cost of electricity has been summarised with an estimated LCOE ranging from 0.062 to 0.86

$/kWh (Branker et al., 2011). Obi et al. (2017) presented a calculation of levelised costs of electricity calculations for various storage systems, specifically pumped hydro, compressed air, and chemical batteries. Pfenninger and Keirstead (2015) compared a large number of cost-optimal future power systems (including solar photovoltaic, nuclear, hydro, offshore wind, fossil fuels etc.) for Great Britain. However, there is a lack of understanding in the problems of evaluating the LCOE values on offshore wind energy.

1.3. Previous developments on LCOE of offshore wind energy

Recently, Allan et al. (2011) indicated the levelised costs of on- and offshore wind are 54.42 and 81.56 £/MWh, respectively. Astariz et al. (2015) performed an evaluation and comparison of the levelised costs of tidal, wave and offshore wind energy. The LCOE values of tidal, wave and offshore wind are 190 €/MWh, 225 €/MWh and 165 €/MWh, respectively. Beiter et al. (2016b) predicted a potential LCOE value of offshore wind below 100 $/kWh at some U.S. coastal sites. Lerch et al. (2018) provided a sensitivity analysis on the LCOE for floating offshore wind farms. The LCOE variation limits obtained in this study vary between 67 €/MWh and 135 €/MWh among different concepts and offshore sites including offshore transmission costs. Voormolen et al. (2016) carried out a study showing that the LCOE value will be increased along with time which is a direct result of the CAPEX increase, the development of average LCOE is shown to increase from 120 €/MWh in 2000 towards 190 €/MWh in 2014. In the meantime, Wiser et al. (2016) pointed out that increasing the turbine size could help reducing the LCOE value. In recent time, based on the work done by Bjerkseter and Ågotnes (2013), Myhr et al. (2014) performed a levelised cost of energy analysis for offshore wind farms. Ioannou et al. (2018a) demonstrated a life cycle cost/revenue model, which is decomposed further into CAPEX, OPEX and. FinEX components and applied for different investor classes based on wind farms operated in European countries. Ioannou et al. (2018b) then performed a parametric CAPEX, OPEX and and LCOE expressions for offshore wind farms based on a North Sea development. Recently, Maienza et al. (2020) developed a life cycle cost model for floating offshore wind farms which provides a life cycle cost model for floating offshore wind farms. To date, most of the LCOE analysis is still based on general assumptions without detailed cost breakdowns and some of the sources are not identified directly.

Regarding the cost breakdown structure, Castro-Santos and Diaz-Casas (2014) evaluated the cost breakdown structure of a floating offshore wind farm. Gonzalez-Rodriguez

(2017) carried out a review of offshore wind farm cost components, the sources are accurately identified, including pages where data were found and the price in the original currency. However, both of the two studies are focused on the cost breakdown structures, the LCOE value has not been provided in their research.

In addition, as Europe is a frontrunner of offshore wind development, studies related to life cycle analysis are mostly based on the experience in Europe. Outside Europe, Mattar and Guzmán-Ibarra (2017) studied the LCOE in Chile with an outcome of the LCOE values between 100 and 114 $/MWh. Beiter et al. (2016b) produced an general estimation of LCOE values for the overall U.S. offshore wind development.

1.4. Limitations of current LCOE analysis in the U.S.

Over the years, several LCOE analysis (Bjerkseter and Ågotnes, 2013; Castro-Santos and Diaz-Casas, 2014, 2015; Gonzalez-Rodriguez, 2017; Guezuraga et al., 2012; Myhr et al., 2014; Tremeac and Meunier, 2009) have been developed as discussed in the above section. As offshore wind energy is an emerging renewable energy market in the U.S., there are still some limitations existed with the evaluation of LCOE values.

- The LCOE analysis is still based on a virtual site development with very general assumptions. The results of such an analytic approach are destined to overly rely on assuming a large scale offshore wind farm installed and operated in a virtual place. There is a lack of data of the LCOE values for the on-going projects.
- Most of the studies related to life cycle analysis are still based on experience in Europe. The cost breakdown and electricity generation outside Europe have not been well addressed yet. This may lead to a wrong LCOE prediction.
- The area/space of offshore wind farm has been ignored when discussing the LCOE values. Previously research on offshore wind farm LCOE generally eliminated the wind farm area issues. However, for a near-shore wind farm, the available coastal area is still limited to the seabed conditions, local government policy and marine transportation. Therefore, the effects of offshore wind farm area still need to be studied.

1.5. Research motivation and scope

The scope of the present work aims to apply the European offshore wind development experiences to a potential U.S. offshore wind farm. Increased offshore knowledge through experience in Europe has led to the development of offshore wind farm in the United States. An initial review of the offshore wind farm investment is provided to evaluate the economic potential of the development and a benchmark wind farm case has been set based on a potential offshore wind development announced by the New York State [4]. To specify the wind farm, three wind farm concepts (based on different rated power offshore wind turbines) are developed at different locations around the New York State offshore area. The offshore wind farm is constructed with bottom-fixed wind turbines. The knowledge of previous developments in Europe is applied to the present study and specific conditions are further considered in accordance with the U.S. regulations, e.g. Section 27 of the Merchant Marine Act (known as the Jones Act) (2006). Additionally, a ten-year observation (2008 - 2017) of the wind speed at the coastal area around New York State (Center, 2018) is applied to predict the offshore wind farm energy generation. In addition, the occupied areas (excluding substations) of the wind farms are considered in the present study. The outcomes of the present study will provide a good insight into the economic potential of future large offshore wind farm developments in the United States.

This paper is aimed to enhance the general understanding of the LCOE analysis for an on-going potential development project in the United States. A robust study on the LCOE value with a rigorous calculation process is presented. All the sources for the cost breakdown and electricity generation are clearly identified. Additionally, the wind farm area effect is raised in the present study for the first time. It is believed that the research findings not only present general understanding of the LCOE values on offshore wind development for stakeholders, but also provide them with an insight into the decision-making process.

2. Methodology

Based on the experiences from European developments, the present work is targeted to develop a method to provide the LCOE analysis for the U.S. offshore wind energy sector. This section provides the methodology (Figure 1) to evaluate the LCOE analysis.

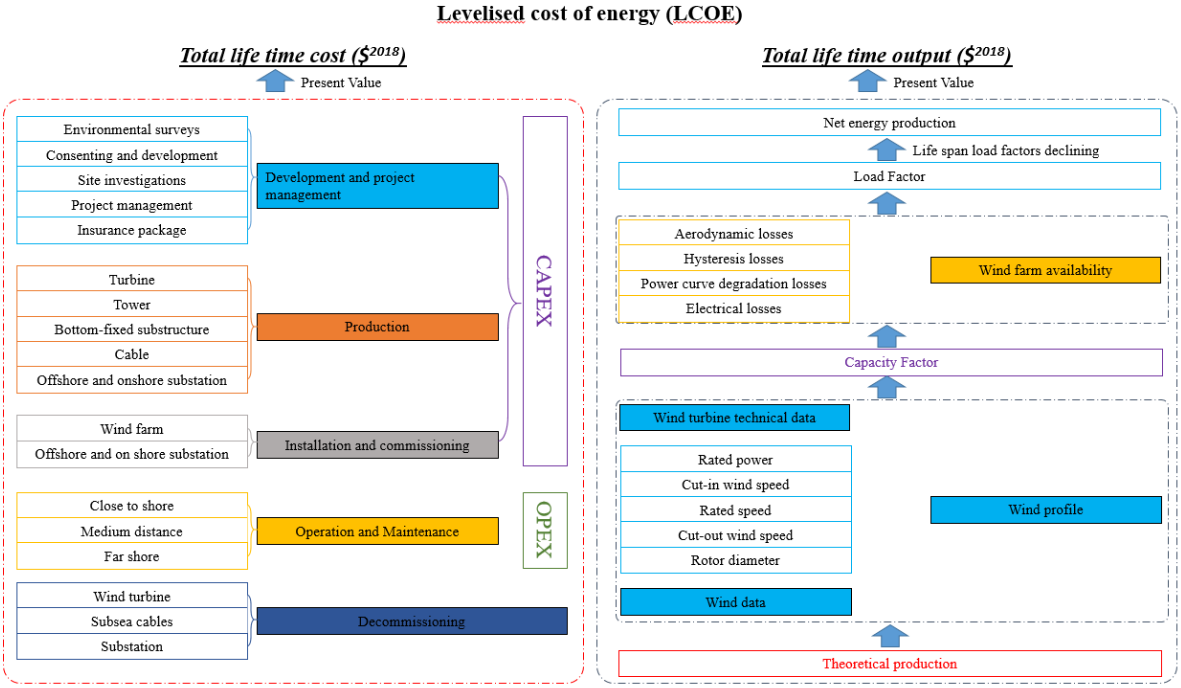

Figure 1. Outline of the present LCOE analysis.

2.1. Levelised Cost of Energy

The LCOE analysis evaluates results from the life cycle cost assessment with regards to measuring lifetime costs divided by energy production. It has been widely accepted to analyse the life cycle or levelized cost (Allan et al., 2011; Lai and McCulloch, 2017). The LCOE may be interpreted as the minimum unit price (discounted to present day prices) for which energy has to be sold in order to break even on the total investment (Veatch, 2010), and the formula for calculating the LCOE is written as (Agency, 2012):

$$LCOE = \frac{Total\ Lifetime\ Cost}{Total\ Lifetime\ Output} = \frac{\sum_{t=0}^{n} \frac{I_t + M_t}{(1+r)^t}}{\sum_{t=0}^{n} \frac{E_t}{(1+r)^t}} \quad (1)$$

where *LCOE* is the average lifetime levelised cost of energy generation, I_t is the investment expense at time t, M_t is the operation and maintenance costs at time t, t is the time, r is the evaluation discount rate, E_t is the energy generated at time t.

2.2. Evaluation discount rate

To perform an LCOE analysis, it is very important to evaluate future costs at a suitable time value. Thus, a discount rate should be performed within the evaluation process, which is the r shown in Eq. (1). In the present study, the discount rate is used as the Weighted

Average Cost of Capital (WACC). Since the present investigation is a site-specific case study, the site-specific WACC is calculated based on a report from the National Renewable Energy Laboratory (Beiter et al., 2016a):

$$WACC = \frac{1+(1-DF)\cdot(RROE\cdot i-1)+DF\cdot(IR\cdot i-1)(1-TaxRate)}{i} \tag{2}$$

where *DF* is the debt fraction (fraction of capital financed with debt); *RROE* is the rate of return on equity (rate of return on the share of assets financed with equity); *i* is the inflation rate (assumed inflation rate based on historical data); *IR* is the interest rate (interest rate on debt); *TaxRate* is the tax rate combined state and federal tax rate.

These parameters can be varied by changing the target site in different regions. In the current study, the values used were, *DF* = 50%, *RROE* = 10%, *i* = 2.5%, *IR* = 5.4%, *TaxRate* = 40% (Beiter et al., 2016a). Based on these values a real WACC of 8.06% was calculated and used in the present work. According to the review carried out by Bjerkseter and Ågotnes (2013), renewable energy projects have a real WACC of 8.2%, thus a good agreement has been observed between the present evaluation and previous outcomes.

2.3. Present Value and Monetary Values

Present value (PV) is the value of an expected income stream determined as of their reference time valuation. The PV is calculated as

$$PV = \frac{C}{(1+r)^t} \tag{3}$$

where, PV is the present value; *C* is the future amount of money at time *t*, *r* is the discount rate and *t* is the time between the present date and the future.

All monetary values are stated in U.S. Dollars ($), and converted to January 2018 values before inflation by the (Industrial) Producer Price Index (PPI).

3. Total time life output

3.1. General reference wind farm assumptions

The wind farm potential scenarios consist of 100 wind turbines for each of the three wind turbine concepts (illustrated in section 3.2). The distance from shore to the wind farm is set to 32, 73 and 160 km respectively for all investigated concepts, at a water depth of 20 ~ 40 m (with an average value of 30 m (NOAA/OER, 2002)). Based on the average water depth, the monopile bottom-fixed structure is employed in the current work. The wind farm is set up as a square formation (10 × 10) with an inner distance between each turbine of 7*D* (where *D* is the diameter of the rotor), as shown in Figure 2. In addition, an offshore substation has been considered in the development plan, which is 1 km away from the wind farm.

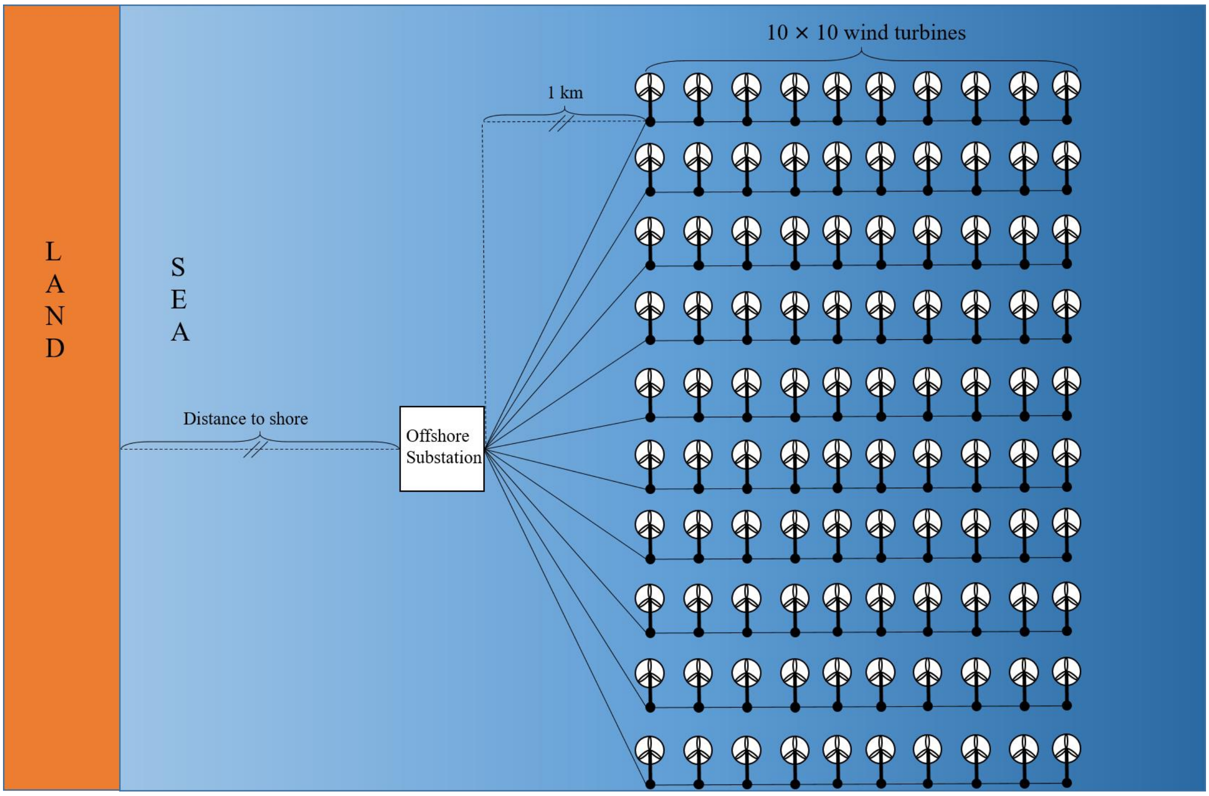

Figure 2 Layout of the potential wind farm scenarios.

Table 1 Site assumptions for the potential wind farm scenarios.

General site assumptions for the offshore wind farm	
Year of development	2018-2023
Commissioning year	2023
Project life span (years)	25
Decommissioning year	2048-2050

Table 2 Technical data for the potential wind farm scenarios.

Technical data for the offshore wind farm	
Number of wind turbines (units)	100
Size of the wind farm (MW)	330, 508 and 800
Average water depth (m)	30
Distance to the nearest port (km)	32, 73 and 160
Turbine operation height (m)	85, 95, 105 and 115
Site soil condition	Medium clay

The general assumptions of the project plan and the technical data for the investigated offshore wind farms are illustrated in Table 1 and Table 2 respectively.

3.2. Offshore wind turbine

Three different rated power wind turbines are investigated in the present work. The details of the wind turbines are illustrated in Table 3, while the power curves for the three different wind turbines (A/S, 2013; AG; AG) are given in Figure 3.

Table 3 Technical data for three wind turbines.

	Vestas V112-3.3 MW (A/S, 2013)	**Repower 5M (AG; AG)**	**Vestas V164-8.0 MW (A/S, 2013)**
Rated power (MW)	3.3	5.075	8.0
Cut-in wind speed (m/s)	3	3.5	4
Rated wind speed (m/s)	12.5	14	13
Cut-out wind speed (m/s)	25	30	25
Rotor diameter (m)	112	126	164
Rotor and nacelle mass (tons)	192.7	350	495

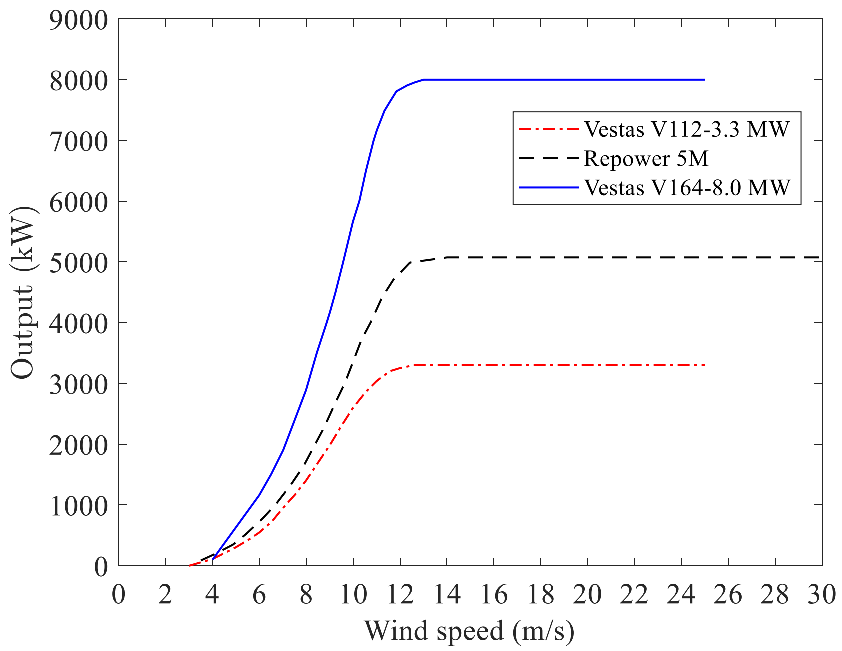

Figure 3 Power curves for three different wind turbines.

3.3.Wind Profile

In the present analysis, the prediction of the offshore wind turbine energy generation was carried out with a ten-year observation (from 2008 to 2017) of the 10-minute average wind speed at the New York State offshore area provided by the National Oceanic and Atmospheric Administration's National Data Buoy Center (Center, 2018). It is noted that wind electricity production is not only affected by average wind speeds but also by, turbulence, wind shear and gusts. Wagner et al. (2010) indicated that, for typical values, the direction shear has a smaller effect on the turbine power output than the speed shear. For example, at a wind speed of 8 m/s, with shear inflow, the power output will have 5% deduction based on the simulation from HAWC2Aero (Wagner et al., 2010). In addition to shear, turbulence level also affects the power generation. Lubitz (2014) pointed out that, for a small wind turbine, low turbulence intensity ($TI < 0.14$) was associated with a 2% decrease in power output in the normal operating range (4 m/s to 7 m/s) relative to power output over all turbulence conditions. Conversely, medium and high turbulence intensity ($TI > 0.14$) was associated with a power increase of approximately 2% in this range. Thus, it is hard to quantify the turbulence effect on the power output. In the current study, only 5% shear effect is accounted for and the effects from turbulence and gusts are not considered.

As mentioned above, ten-year historical data (from 2008- 2017) of 10-minute average wind speeds are provided by National Data Buoy Center (Center, 2018) at the assumed development place. Data collected from three sites are used in the current investigation at the target offshore wind farm development locations (see Table 4).

Table 4 Wind speed observation site information

Site	**A**	**B**	**C**
NDBC Station ID	44065	44025	44066
Type	3-meter discus buoy	3-meter discus buoy	3-meter discus buoy
Location	40°22'10" N 73°42'10" W	40°15'3" N 73°9'52" W	39°34'6" N 72°35'8" W
Distance to port (km)	32	73	160
Anemometer height (m), above sea level	4	5	5

It is noted that all anemometers listed in Table 4 are only placed a few meters over the sea level. To transfer the wind data from the anemometer to the hub height of the wind turbine, the 1/7 power law is employed. Four different operation hub heights are considered, varying from 85 m to 115 m and spacing by 10 m (as shown in Table 2). In the rest of the present study, all the average wind speeds are specified as the wind speed at hub height.

3.3.1. Seasonal wind profile

Based on the ten-year historical observations, seasonal wind profiles have been further analysed to illustrate the performance via seasonal bias. In the present study, the calendar year is divided into four quarters, abbreviated as Q1 (1st January – 31st March), Q2 (1st April – 30th June), Q3 (1st July – 30th September) and Q4 (1st October – 31st December). Probability density function is employed to illustrate the wind speed distribution. From Figure 4, Figure 5 and Figure 6, it can be observed that there is a huge difference in the wind speed distribution between Q1, Q4 and Q2, Q3. In Q1 and Q4, the majority of the wind speeds locate within the range of 10 ~ 15 m/s. However, in Q2 and Q3, most of the wind speeds locate within the range of 5 ~ 10 m/s, which are much lower than Q1 and Q4.

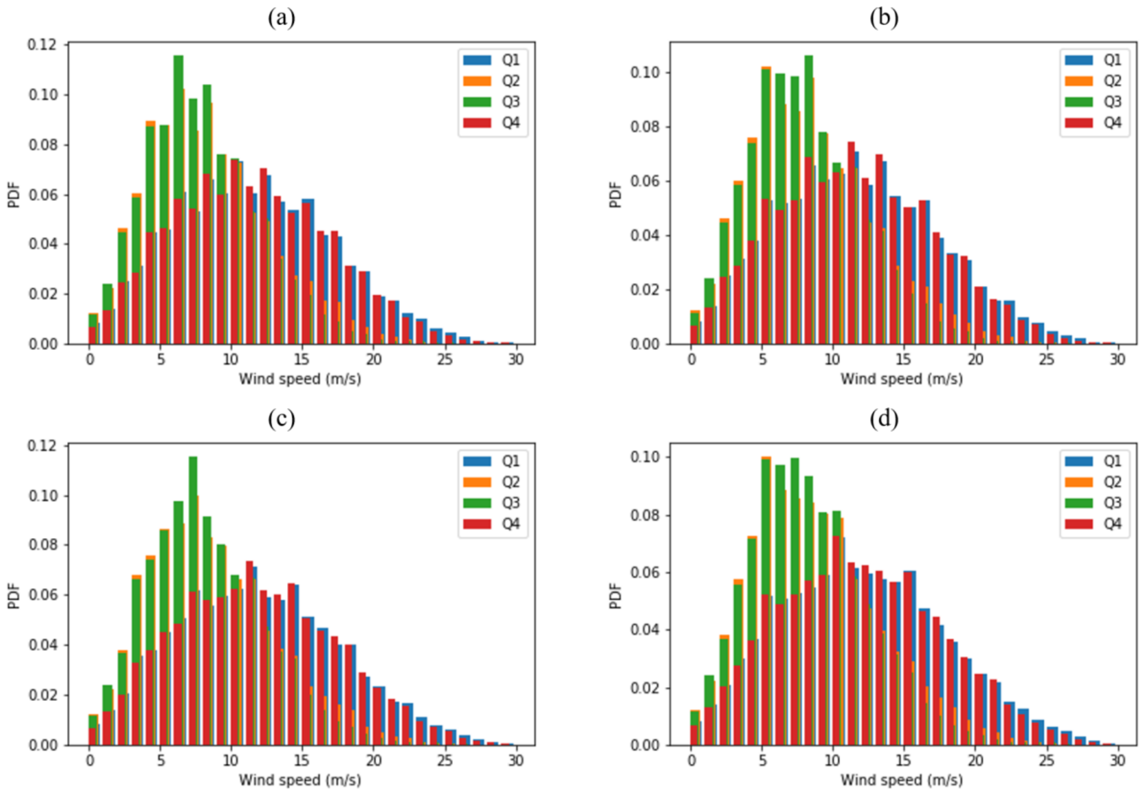

Figure 4 Probability density function (PDF) of wind speed at different hub height for Site A: (a) hub height at 85 m; (b) hub height at 95 m; (c) hub height at 105 m; (d) hub height at 115 m.

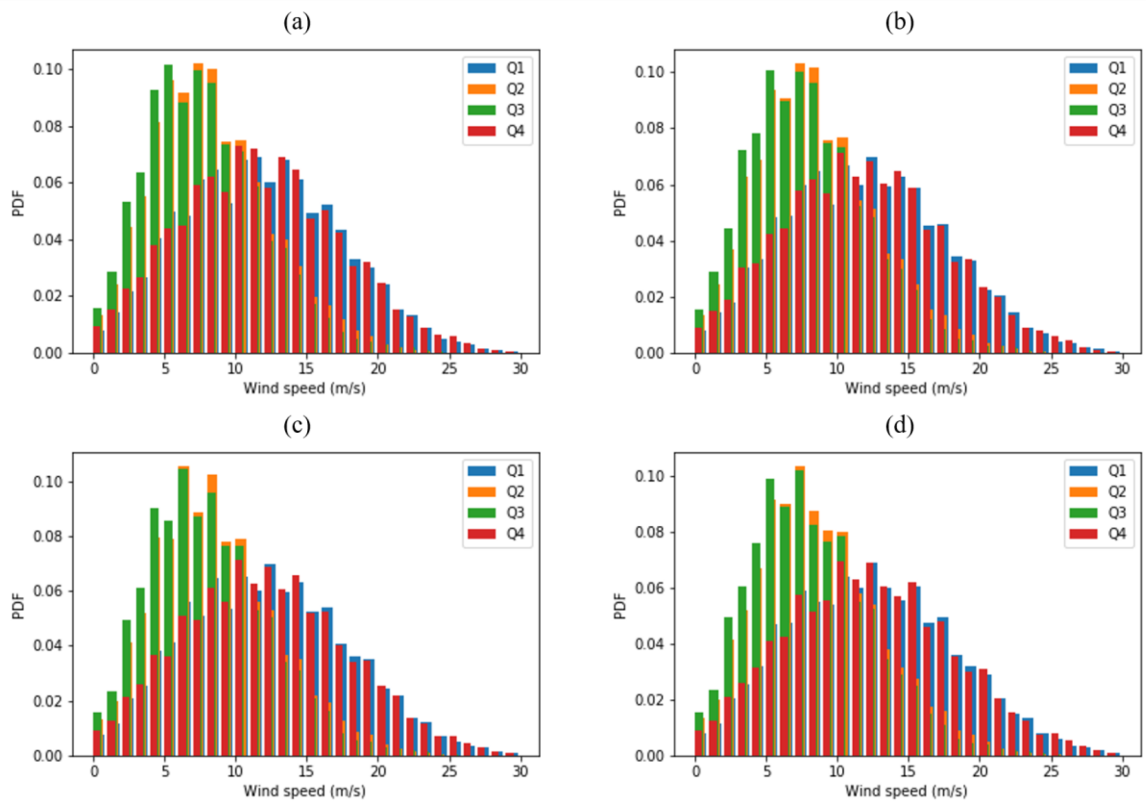

Figure 5 Probability density function (PDF) of wind speed at different hub height for Site B: (a) hub height at 85 m; (b) hub height at 95 m; (c) hub height at 105 m; (d) hub height at 115 m.

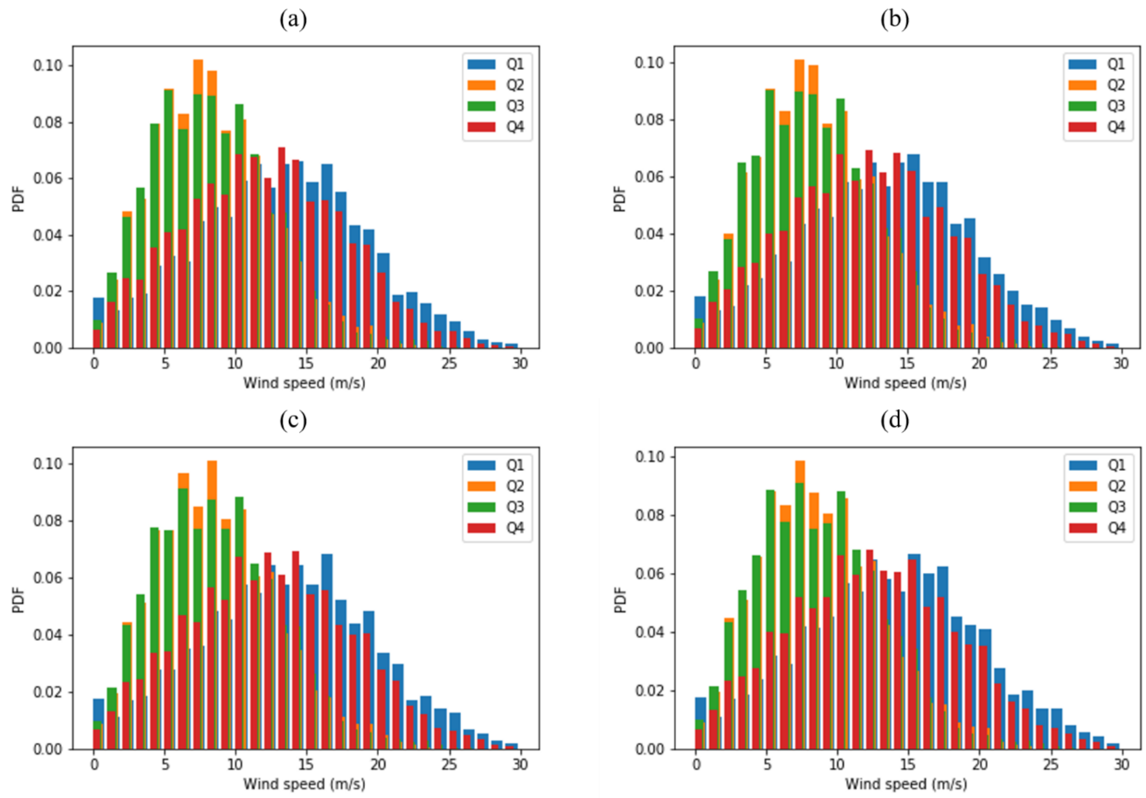

Figure 6 Probability density function (PDF) of wind speed at different hub height for Site C: (a) hub height at 85 m; (b) hub height at 95 m; (c) hub height at 105 m; (d) hub height at 115 m.

3.3.2. Capacity factor based on the 10-year observation.

To date, most of the LCOE of wind turbine analysis is based on the capacity factor for evaluating wind electricity production. The capacity factor is defined as the ratio between anticipated electricity production and theoretical production if the turbine was to operate at rated power throughout a year. According to the data provided by OpenEI (2019), historical data published from 2007 to 2015 showed that the maximum capacity factor of offshore wind is 54%. In addition, other researchers, such as Bjerkseter and Ågotnes (2013) provided a capacity factor of 53% for a 5 MW offshore wind turbine. In the current work the capacity factor is calculated using the historical wind data for the 3 types of wind turbines.

Table 5 Capacity factor at Site A.

Vestas V112-3.3 MW				
Operation height (m)	85	95	105	115
Capacity Factor (%)	61.2	62.0	62.7	63.4
Repower 5M				
Operation height (m)	85	95	105	115
Capacity Factor (%)	53.1	54.0	54.9	55.5
Vestas V164-8.0 MW				
Operation height (m)	85	95	105	115
Capacity Factor (%)	53.1	54.0	54.6	55.2

Table 6 Capacity factor at Site B.

Vestas V112-3.3 MW				
Operation height (m)	85	95	105	115
Capacity Factor (%)	60.8	61.7	62.4	63.1
Repower 5M				
Operation height (m)	85	95	105	115
Capacity Factor (%)	52.9	53.8	54.6	55.3
Vestas V164-8.0 MW				
Operation height (m)	85	95	105	115
Capacity Factor (%)	52.8	53.6	54.3	54.9

Table 7 Capacity factor at Site C.

Vestas V112-3.3 MW				
Operation height (m)	85	95	105	115
Capacity Factor (%)	66.3	67.1	67.6	68.1
Repower 5M				

Operation height (m)	85	95	105	115
Capacity Factor (%)	58.6	59.5	60.2	60.9
	Vestas V164-8.0 MW			
Operation height (m)	85	95	105	115
Capacity Factor (%)	58.1	58.7	59.3	59.8

As shown in Table 5, Table 6 and Table 7, by considering the wind speed and shear effect (apart from gust and turbulence), the capacity factor increases by increasing the operation height and the distance from the shore. It is further noted that, the capacity factors are decreased by increasing the rated power of the wind turbine. In addition, the difference in the capacity factors between the wind turbines can be related to the rated speed beside the rated power. However, the rated speed of turbines may vary from different turbine supplier. Thus, the calculation of the capacity factor is suggested to consider the power coefficient curve, cut-in and cut-our speed as well as the turbine diameter in future.

Myhr et al. (2014) carried out an LCOE analysis with a capacity factor of 53 ± 3 % for a 5 MW turbine with a distance of 200 km to port. In the present study, at Site C (160 km to port), a capacity factor of 58.6% at 85 m hub height is observed, which is quite close to the results provided by Myhr et al. (2014).

3.4.Wind farm availability

Wind farm availability denotes the average percentage of time that the wind turbine will operate and is often assumed between 95% (Bjerkseter and Ågotnes, 2013) and 98% (Association, 2009). For a bottom fixed substructure, Beiter et al. (2016a) developed an equation to estimate the annual availability based on the distance to port, which is shown below:

$$\text{Annual Ava (\%)} = 6 \times 10^{-8} \cdot {D_p}^2 - 2 \times 10^{-5} \cdot D_p + 0.9211 \qquad (4)$$

where, D_p is the distance from port to project site

Under a moderate metocean condition, the result of calculated annual availability is shown in Table 8. As seen in Figure 7, based on Eq (4), the annual availability with a distance from 75 km to 150 km is close to 92%. And it starts to increase over 200 km. It is noted that the availability rate under a mild or a moderate metocean condition is quite similar. However, server metocean condition can decrease the availability around 5% compared with the moderate condition (Beiter et al., 2016a). In addition, wind resource increases along with the distance from port. And the downtime of the site as well as the maintenance time can varied with the distance from the port. Unlike the shallow water region, the O&M procedure becomes more similar in the deepwater region (Beiter et al., 2016a). Therefore, deepwater regions benefit from the rich wind resources.

Table 8 Annual availability with different distance to port (Beiter et al., 2016a).

Site	**A**	**B**	**C**
Annual Availability (%)	92.1	92.0	92.0

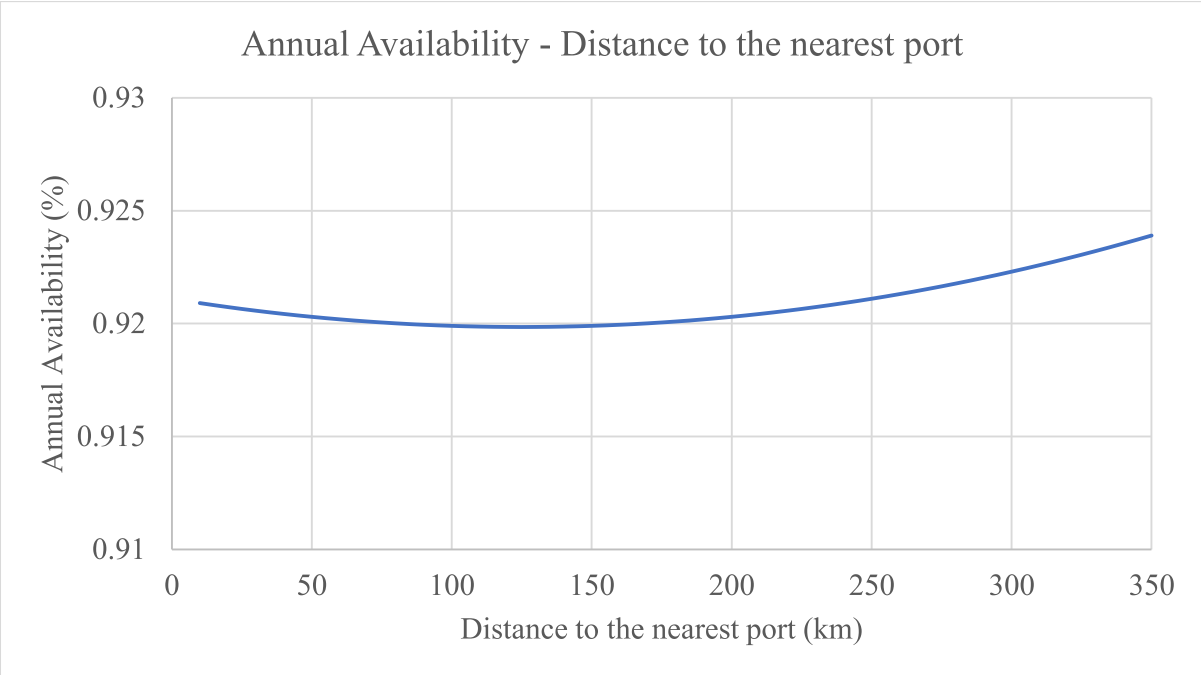

Figure 7 Annual availability against the distance to the nearest port.

3.5.Aerodynamic losses

Aerodynamic losses, also known as the wake effect, relates to the wind turbine being affected by other turbines' wake in a wind farm, leaving less energy in the downstream. The Association (2009) indicated that this loss may account for 5 ~ 10 % of the output, with an average of 7.5%. Thus, an aerodynamic losses factor of 7.5% is used in the present work.

3.6.Hysteresis losses

Hysteresis losses are losses coming from rapid changes in wind direction to such an extent that the yaw mechanism of the wind turbine may not sufficiently and efficiently keep up with it. According to the Association (2009), the hysteresis losses is estimated as 1%. Thus, a hysteresis losses factor of 1% is used in the current work.

3.7. Power curve degradation losses

Diminishing of power performance through soiling effects has potentially severe negative effects on offshore wind turbines. When taking soiling from dust or corrosion into account, power performance losses have been estimated as 2% (Association, 2009). Thus, a power performance losses factor of 2% is used in the present work.

3.8. Grid connections and electrical losses

When power is transferred within the wind farm, electrical losses will be generated due to the resistance of the cable.

Current losses in a cable are given by:

$$P_{loss} = I^2 \cdot R \tag{5}$$

where, P_{loss} is the ohmic power losses, *I* is the grid current, *R* is the cable resistance.

$$R = \frac{\rho l}{A} \tag{6}$$

where, ρ is the material-specific electrical resistivity, 1.75×10^{-8} Ωm; *l* is the cable length, *A* is the cable cross-sectional area.

$$I = \frac{P}{\sqrt{3}E} \tag{7}$$

where, *P* is the active power of the turbine and *E* is the transformer voltage.

There are mainly two basic types of cable used in an offshore wind farm which will cause electrical losses: inter-array cable and export cable.

3.8.1. Inter-array cable

Within the inter-array, the voltage must stay the same, resulting the current to increase with the same factor along with the power. The demonstrated current distribution is shown in Figure 8.

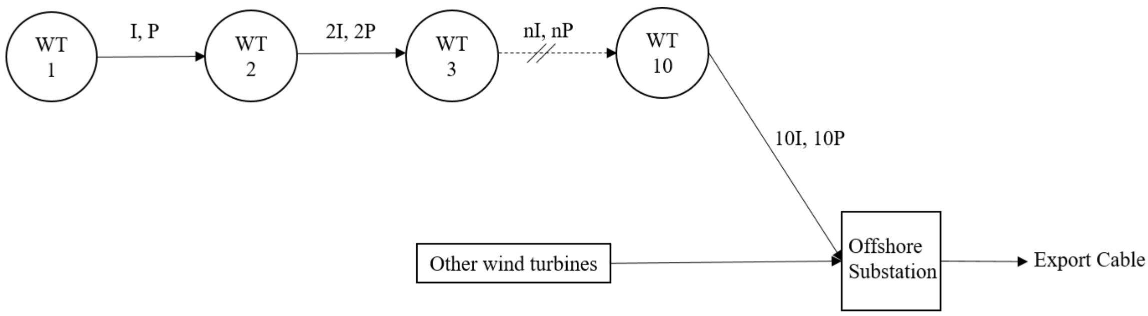

Figure 8 Power and current within the inter-array.

The present investigated inter-array structures are illustrated in Figure 2. The inter-array structures are simplified to provide a reasonable cable consumption and corresponding electrical array losses. The towers are connected on one side of the substation in a series of ten, with a total of ten rows. To avoid damages due to cable tension and to simplify the cable installation, the cable length between each turbine or between turbine and substation is set as 1.6 times (Bjerkseter and Ågotnes, 2013) of the distance between them. The inter-array cable provided in the present work is a 33 kV copper cable (300 mm^2). The electric loss within the inter-array cable is significantly affected by the type of wind turbine installed in the wind farm. Table 9 illustrates the maximum percentage of power loss within the inner array based on the ideal rated power output. However, this loss factor can be decreased by considering all the power losses from the rated power output. The average percentage of power loss within the inner array cable for the different scenarios are shown in Table 10, Table 11 and Table 12.

Table 9 Maximum power loss within the inner array.

Wind turbine	**Vestas V112-3.3 MW**	**Repower 5M**	**Vestas V164-8.0 MW**
Total cable length (km)	149.395	167.037	215.187
Max power within the inter array (MW)	330	508	800
Max percentage of power loss (%)	0.43	0.73	1.46

Table 10 Average percentage of inner array power loss at Site A.

Vestas V112-3.3 MW				
Operation height (m)	85	95	105	115
Average percentage of power loss (%)	0.11	0.11	0.11	0.12
Repower 5M				
Operation height (m)	85	95	105	115
Average percentage of power loss (%)	0.14	0.15	0.15	0.15

Vestas V164-8.0 MW				
Operation height (m)	85	95	105	115
Average percentage of power loss (%)	0.28	0.29	0.3	0.3

Table 11 Average percentage of inner array power loss at Site B.

Vestas V112-3.3 MW				
Operation height (m)	85	95	105	115
Average percentage of power loss (%)	0.11	0.11	0.11	0.12
Repower 5M				
Operation height (m)	85	95	105	115
Average percentage of power loss (%)	0.14	0.14	0.15	0.15
Vestas V164-8.0 MW				
Operation height (m)	85	95	105	115
Average percentage of power loss (%)	0.28	0.29	0.29	0.3

Table 12 Average percentage of inner array power loss at Site C.

Vestas V112-3.3 MW				
Operation height (m)	85	95	105	115
Average percentage of power loss (%)	0.13	0.13	0.13	0.13
Repower 5M				
Operation height (m)	85	95	105	115
Average percentage of power loss (%)	0.17	0.18	0.18	0.18
Vestas V164-8.0 MW				
Operation height (m)	85	95	105	115
Average percentage of power loss (%)	0.34	0.34	0.35	0.35

3.8.2. Export cable and Offshore Substation

Export cables are usually used to transfer the electricity to the shore with high voltage. In the present study, a 320 kV HVDC extruded cable with a cross-sectional area of 1500 mm^2 [20] is applied. In addition to the cables, the offshore substation (HVDC used in the present study) will also cause electrical losses and the average losses in the substation and export cable are 4.5% according to May et al. (2016).

3.9. Life span load factors declining

According to Staffell and Green (2014), based on the observation from onshore wind farms, wind turbines are found to lose 1.6 ± 0.2% of their output per year, with average load factors declining from 28.5% at start to 21% at age 19. In the present study, as a project life span of 25 years is specified, an annual decrease of 1.6% energy output has been adopted to the total electricity production.

4. Total time life cost

The life cycle cost analysis (LCCA) is presented in this section. It is noted that the present analysis not only considers the investment costs, but also operation and maintenance costs during the lifetime of the project as well as includes the decommissioning cost at the end of the project life span. The current LCCA model has been divided into five sub-sections: 1. Development and project management; 2. Production; 3. Installation and commissioning; 4. Operation and maintenance; 5. Decommission. Details of each sub-sections will be introduced in the following parts.

4.1. Development and project management

According to Enterprise (2016), the development and project management makes up 3% of lifetime expenditure of an offshore wind farm. The breakdown of cost in the development and project management sub-elements are shown in Figure 9.

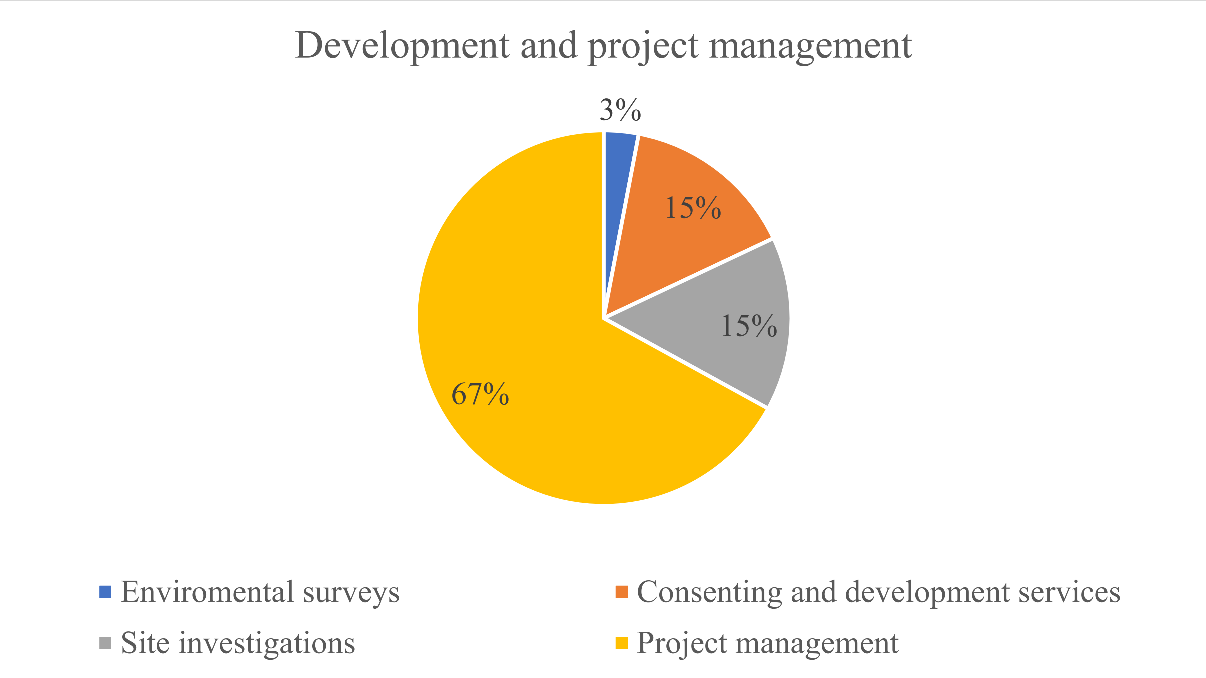

Figure 9 Breakdown of cost in the development and project management sub-elements.

For a 500 MW bottom fixed offshore wind farm, the total costs for development and project management is £^{2016} 158 million (Enterprise, 2016) (\$^{2018} 224.95 million), corresponding to £^{2016} 0.316 million (\$^{2018} 0.450 million) per MW. With an increasing farm capacity, it is expected that the total development and project management will not increase exactly proportional to the farm capacity, however, a linear coherence between capacity and costs is still assumed. In the present study, one additional MW (to increase the capacity by

1MW) for an offshore wind farm is expected to induce an additional development and consenting cost of three-quarters of $\$^{2018}$ 0.45 million. A typical €^{2012} 50,000 ($\$^{2018}$ 59,360) per MW construction phase insurance package is assumed for lowered risk based on the estimation from P.(PVC) (2012). Figure 10 presents the total cost of the development and project management costs.

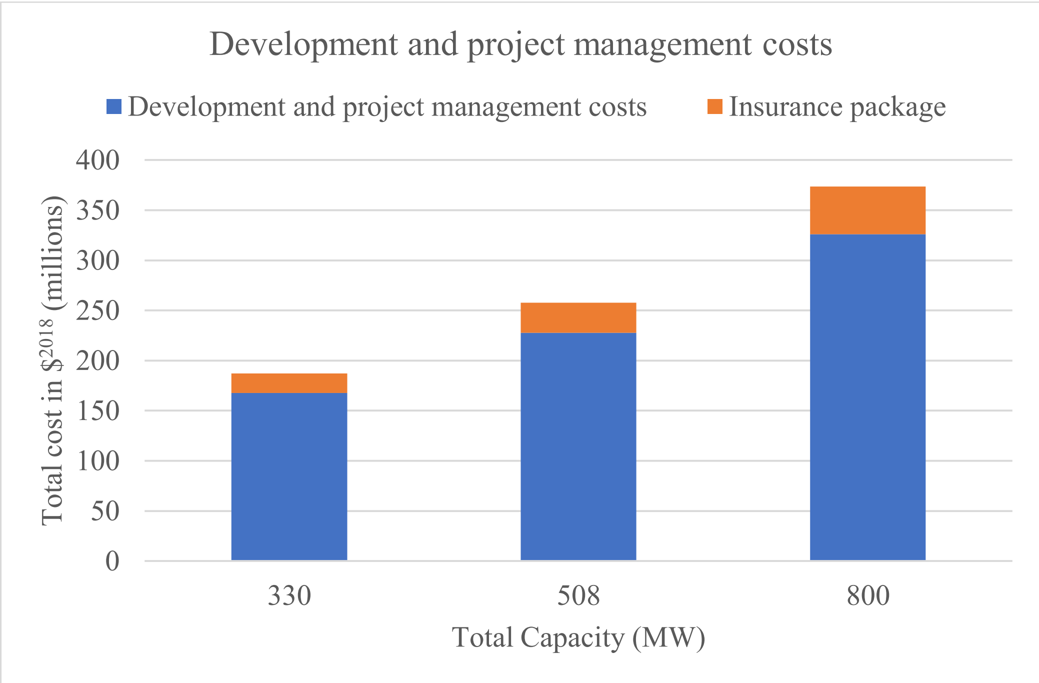

Figure 10 Development and project management costs (inclusive insurance) for three different capacity wind farm.

4.2. Production

This section introduces the capital expenditure from productions, including the turbine, tower, bottom-fixed substructures, cables and substation.

4.2.1. Turbine costs

According to the studies carried out by Agency (2012), The Crown Estate (2010) and Logan (2017), the total turbine costs (exclusive tower) are illustrated in Table 13. It is noted that, in the present study, within one wind farm, the turbine costs are assumed to be constant.

Table 13 3 different rated power turbine costs

Rated Power (MW)	**3.3**	**5.08**	**8**
Turbine Cost ($\$^{2018}$)	4,766,496 (Agency, 2012)	8,032,207 (The Crown Estate, 2010)	9,630,646 (Logan, 2017)

4.2.2. Tower costs

The current work investigates the LCOE under different hub heights ranging from 85 to 115 m. As such, the tower height will change and thus affect the tower cost. In the present analysis, an unmodified NREL 5 MW turbine (Jonkman et al., 2009) is set for calculating the tower cost, in which a 90 m tower has a mass of 347,460 kg (Jonkman et al., 2009) . According to Ancona and McVeigh (, a wind turbine tower contains 98% steel and 2% pre-stressed concrete. Thus, a 90 m tower contains 340,511 kg steel and 6,949 kg pre-stressed concrete. Based on a linear assumption for the material spending on a tower, an assumption of 3,783 kg of steel per meter height and 77 kg of pre-stressed concrete per meter height are used in the present study. According to Bjerkseter and Ågotnes (2013), S355 is used as the present steel with a thickness from 6 ~ 100 mm, width from 2,000 ~ 2,500 mm and length between 8 ~ 15 m. The price of the S355 steel is about $\$^{2018}$ 680 ~ 1,250 per ton.(Alibaba, 2019b), with an average of $\$^{2018}$ 965 per ton. For the pre-stressed concrete, the price is about $\$^{2018}$ 2,500 ~ 2,700 per ton (Alibaba, 2019a), with an average of $\$^{2018}$ 2,600 per ton. A breakdown and total costs for the towers with different heights are listed in Table 14.

Table 14 Breakdown and total costs for the tower with different operation heights.

Tower height (m)	**85**	**95**	**105**	**115**
S335 Steel Cost ($\$^{2018}$)	310,300	346,806	383,312	419,818
Pre-stressed concrete ($\$^{2018}$)	17,017	19,019	21,021	23,023
Total ($\$^{2018}$)	327,317	365,825	404,333	442,841

4.2.3. Bottom-fixed substructure cost

At a water depth of 30 m, the total monopile weight is estimated as 1200 ton (Bjerkseter and Ågotnes, 2013; De Vries et al., 2011) and according to the prediction made by Faaij and Junginger (2004), the production costs of monopile foundations consist roughly of 45 ~ 50 % material costs (steel), and 50 ~ 55% of production costs. In the present study, an average of 52.5 % of production costs is employed (see Table 15).

Table 15 Cost breakdown for a single monopole substructure

Bottom-fixed substructure type	**Monopile**
Material (steel in tons)	1,200
Material costs ($\$^{2018}$)	1,158,000
Production costs ($\$^{2018}$)	1,279,895
Total costs ($\$^{2018}$)	2,437,895

4.2.4. Cable cost

As mentioned in the section 3.8, there are mainly two basic types of cable used in an offshore wind farm: inner array cables and export cable. The costs for a 33 kV AC array cable (300 mm^2) is approximately \$^{2018} 38,598 per km (Bjerkseter and Ågotnes, 2013) and the total cost of the inter-array cables is presented in Table 16.

Table 16 Total inter-array cable cost for different capacity wind farms.

Wind farm capacity (MW)	**330**	**508**	**800**
Inter-array cable cost (\$^{2018})	5,766,348	6,447,294	8,305,787

In addition to inner array cable, a 320 kV HVDC extruded cable with a cross-sectional area of 1500 mm^2 has been employed as the export cable. The costs for this cable is \$^{2018} 537,767 per km (Grid, 2011). Since the operation site distance is varied in the present work, the cost of export cable with different distances from the port are listed in Table 17.

Table 17 Total cost for the export cables.

Site	**A**	**B**	**C**
Distance from port (km)	32	73	160
Export cable cost (\$^{2018})	17,208,544	39,434,454	860,428,320

4.2.5. Offshore and onshore substation

Apart from the wind turbine and cables, the substation cost is also a main contributor during the production phase. An offshore substation (HVDC) usually includes AC switchgear, transformers, converter electronics and filters. Based on the report published by Grid (2011), the converter and the substation platform are the main cost drivers for a substation. For a wind farm of 330 MW capacity, a 400 MW bottom fixed offshore substation is employed. A 500 MW bottom fixed offshore substation is used for a 508 MW wind farm. And a 1000 MW bottom fixed offshore substation is applied for an 800 MW wind farm. As the export cable is HVDC, the onshore substation will convert the power to three-phase AC and based on The Crown Estate (2010), the cost for an onshore substation is approximately half of the cost of the offshore bottom-fixed substation. The total cost of a substation is listed in Table 18.

Table 18 Total cost of the substation (Bjerkseter and Ågotnes, 2013; The Crown Estate, 2010).

Wind farm capacity (MW)	**330**	**508**	**800**
Offshore substation cost (\$^{2018})	139721728.5	169825815.9	279847312.1

Onshore substation cost ($^{2018})	69860864.23	84912907.95	139923656.1

4.3. Installation and commissioning

Castro-Santos et al. (2018) provides a methodology to calculate the installation costs of offshore wind farms in deep waters, and Beiter et al. (2016a) demonstrated a methodology to present the installation cost in the U.S coast area. As the present study is focused on a development based in the U.S. The methodology provides by Beiter et al. (2016a) is applied.

The substructures are assumed to be loaded onto an installation vessel at the staging port for transportation to the project site where the substructures will be installed. The turbine installation is performed in a similar fashion. The turbine components (blade, nacelle, tower etc.) are loaded onto the installation vessel at the staging port, transported to the project site, and then assembled and installed onto the preinstalled substructure at the site (Beiter et al., 2016a).

Three reference wind farms' (consisted of 3 MW, 6 MW and 10 MW) installation and commissioning cost is calculated using the following set of equations (Beiter et al., 2016a),:

For a 3 MW monopile offshore wind turbine:

$$C_s = 86671670 - 3230771 \cdot W_d + 3918 \cdot D_p + 112670 \cdot W_d^2 + 2.23e^{-8} \cdot D_p^2 + 225 \cdot W_d \cdot D_p - 760 \cdot W_d^3 - 2.95e^{-11} \cdot D_p^3 + 6.43e^{-11} \cdot W_d \cdot D_p^2 + 22.9 \cdot W_d^2 \cdot D_p \quad (8)$$

$$C_t = 31368338 - 89169 \cdot W_d + 65674 \cdot D_p + 13557 \cdot W_d^2 - 4.13e^{-8} \cdot D_p^2 - 1485 \cdot W_d \cdot D_p - 100 \cdot W_d^3 + 6.84e^{-11} \cdot D_p^3 + 2.2e^{-10} \cdot W_d \cdot D_p^2 + 9.34 \cdot W_d^2 \cdot D_p \quad (9)$$

$$C_{ps} = 6419595 + 31553 \cdot W_d - 5364 \cdot W_d^2 + 189 \cdot W_d^3 - 2.27 \cdot W_d^4 + 0.009 \cdot W_d^5 + 6622 \cdot D_p \quad (10)$$

For a 6 MW monopile offshore wind turbine:

$$C_s = 88705573 - 2965980 \cdot W_d - 7813 \cdot D_p + 104665 \cdot W_d^2 + 1.49e^{-6} \cdot D_p^2 + 661 \cdot W_d \cdot D_p - 707 \cdot W_d^3 - 1.71e^{-9} \cdot D_p^3 - 2.75e^{-11} \cdot W_d \cdot D_p^2 + 19.44 \cdot W_d^2 \cdot D_p \quad (11)$$

$$C_t = 15687102 + 2685414 \cdot W_d - 149549 \cdot W_d^2 + 3474 \cdot W_d^3 - 34.1 \cdot W_d^4 + 0.12 \cdot W_d^5 + 3133853 \cdot \ln D_p \quad (12)$$

$$C_{ps} = 7136675 - 21122 \cdot W_d + 1336 \cdot D_p + 449 \cdot W_d^2 + 0.009 \cdot D_p^2 + 58.2 \cdot W_d \cdot D_p \quad (13)$$

For a 10 MW monopile offshore wind turbine:

$$C_s = 1.7686e^8 - \frac{2.26e^6}{W_d} + 257702 \cdot D_p + \frac{1.21e^{10}}{W_d^2} + 1.82e^{-8} \cdot D_p^2 - 2558888 \cdot \left(\frac{D_p}{W_d}\right) \quad (14)$$

$$C_t = 57108119 + 1166746 \cdot W_d - 58333 \cdot W_d^2 + 1217 \cdot W_d^3 - 10.6 \cdot W_d^4 + 0.032 \cdot W_d^5 + 24987 \cdot D_p \quad (15)$$

$$C_{ps} = \frac{7533930 - 116296 \cdot W_d + 1084 \cdot W_d^2 - 1.22 \cdot W_d^3 - 1425 \cdot D_p}{1 - 0.013 \cdot W_d + 8.83 \cdot e^{-5} \cdot W_d^2 - 0.0005 \cdot D_p + 2.38e^{-7} \cdot D_p^2} \quad (16)$$

where:

C_s is the turbine installation cost

C_t is the substructure installation cost

C_{ps} is the port and staging cost

D_p is the distance from staging port to project site (km)

W_d is the maximum water depth at project site (m)

To estimate costs between the range of turbine sizes from 3 ~ 10 MW, a linear interpolation was developed by Beiter et al. (2016a), following with the equation:

$$x_c = \begin{cases} \left|\frac{TR-3}{3}\right| \cdot C_6 + \left|\frac{TR-6}{3}\right| \cdot C_3, & 3 \le TR \le 6 \\ \left|\frac{TR-6}{4}\right| \cdot C_{10} + \left|\frac{TR-10}{4}\right| \cdot C_6, & 6 < TR \le 10 \end{cases} \quad (17)$$

where:

x_c is the interpolated installation cost

TR is the turbine rating in megawatts

C_3 is the 3 MW turbine installation cost function

C_6 is the 6 MW turbine installation cost function

C_{10} is the 10 MW turbine installation cost function

Thus, the total costs for installing a turbine under the present investigation are illustrated in Table 19.

Table 19 Offshore wind turbine installation cost with different distances to port.

Site	A	B	C
Distance from port (km)	32	73	160
3.3 MW turbine cost ($\$^{2018}$)	117,744,451	120,647,270	126,434,280
5.08 MW turbine cost ($\$^{2018}$)	122,129,125	125,719,553	131,165,390
8 MW turbine cost ($\$^{2018}$)	97,733,142	103,778,445	114,951,811

Apart from the wind turbine installation, the installation of an offshore substation is also a key factor during the installation phase. According to Bjerkseter and Ågotnes (2013), the present offshore wind farm consists of three configuration: 400 MW bottom fixed substation (for a 330 MW wind farm), 500 MW bottom fixed substation (for a 508 MW wind farm) and 1000 MW bottom fixed substation (for an 800 MW wind farm). The total installation cost of the substation is listed in Table 20.

Table 20 Substation installation cost.

Wind farm capacity (MW)	330	508	800
Offshore substation cost ($\$^{2018}$)	25,769,135.55	28,245,416.11	43,419,177.16
Onshore substation cost ($\$^{2018}$)	12,884,567.78	14,122,708.06	21,709,588.58

In addition, the costs above are mostly summarised based on the European site data. However, Section 27 of the Merchant Marine Act (known as Jones Act) (2006) in the U.S. stipulates that only U.S.-flagged vessels can make consecutive trips from one U.S. port to another. Thus, a Jones Act Factor of 23% increase to the installation cost is added before 2020 (Beiter et al., 2016a), and for 2030 the value will become 5% (Beiter et al., 2016a). In the present work, a linear assumption for the Jones Act Factor between 2020 and 2030 has been used. By 2033, the Jones Act Factor will then become 0%.

4.4. Operation and Maintenance

Three strategies developed by Beiter et al. (2016a) were employed in the present study (see Table 21). It is noted that the present study assumes that all vessels are chartered and no capital investment is required.

Table 21 Operation and Maintenance Strategy (Beiter et al., 2016a).

Strategy	Close to Shore +	Medium Distance	Far Shore
Principle Access Vessel	Advanced Crew transfer vessel	Surface effect ship	Crew transfer vessel with mothership support
Distance to Port (km)	<= 65	65< x <150	> 150
Wind limit (m/s)	20	20	20
Hs limit (m/s)	2.3	2.5	2.5
Access Vessel Day Rate ($, 2016)	6500	9000	2800
Vessel Speed (kn)	20	35	20
Passengers	12	12	12
Shift Length (h)	12	12	23
Docking and Transfer Time (h)	0.5	0.5	1.0
Fuel Consumption Rate (gal/h)	25	20	25
Fixed Annual Maintenance Cost ($^{2018})	na	na	18000000

In the present study, the OPEX is estimated under a metocean condition with a significant wave height, H_S = 1.39 m and mean wind speed, W_S = 7.32 m/s, and the annual OPEX for different sites is summarised below. It is noted that the OPEX under a mild or a moderate metocean condition is quite similar. However, server metocean condition can increase the OPEX around 5 ~ 10% compared with the moderate condition (Beiter et al., 2016a).In addition, a 1% OPEX for operating phase insurance is further added based on Table 22.

Table 22 OPEX for three different operating sites.

Site	A	B	C
Annual O & M cost (million $^{2018})	88.8	91.8	101
Annual OPEX (inclusive insurance, million $^{2018})	89.7	92.7	102

4.5. Decommissioning

Due to the lack of understanding of offshore wind farm decommission, the present work simplifies the decommissioning cost as a percentage of installation cost based on Myhr et al. (2014) (see Table 23).

Table 23 Relation between the decommissioning cost and installation cost (Myhr et al., 2014).

Wind farm components	Percentage of installation cost
Wind turbine	80
Subsea cables	10

Substation	90

5. Results and Discussion

Based on the methodology and workflow described in the section above, the details of CAPEX, OPEX and LCOE for the offshore wind farms at New York State coastal area in the current study are discussed in this section. In order to have a general overview first, a benchmark case is defined first. Then the sensitivity analysis related to turbine rated power, operation height, site distance to the port and the seasonal performance is conducted. The benchmark case used in the present study is defined in Table 24.

Table 24 Benchmark offshore wind farm case.

Benchmark offshore wind farm	
Year of development	2018-2023
Commissioning year	2023
Project life Span (years)	25
Decommissioning year	2048-2050
Wind turbine type	Repower 5M
Number of wind turbines (units)	100
Size of the wind farm (MW)	508
Average water depth (m)	30
Distance to the nearest port (km)	73
Turbine operation height (m)	105
Site soil condition	Medium clay

5.1. Total capital expenditures

In the present section, the total CAPEX for the benchmark case following with two different rated power turbine wind farms (operated at the same site) are presented in Figure 11.

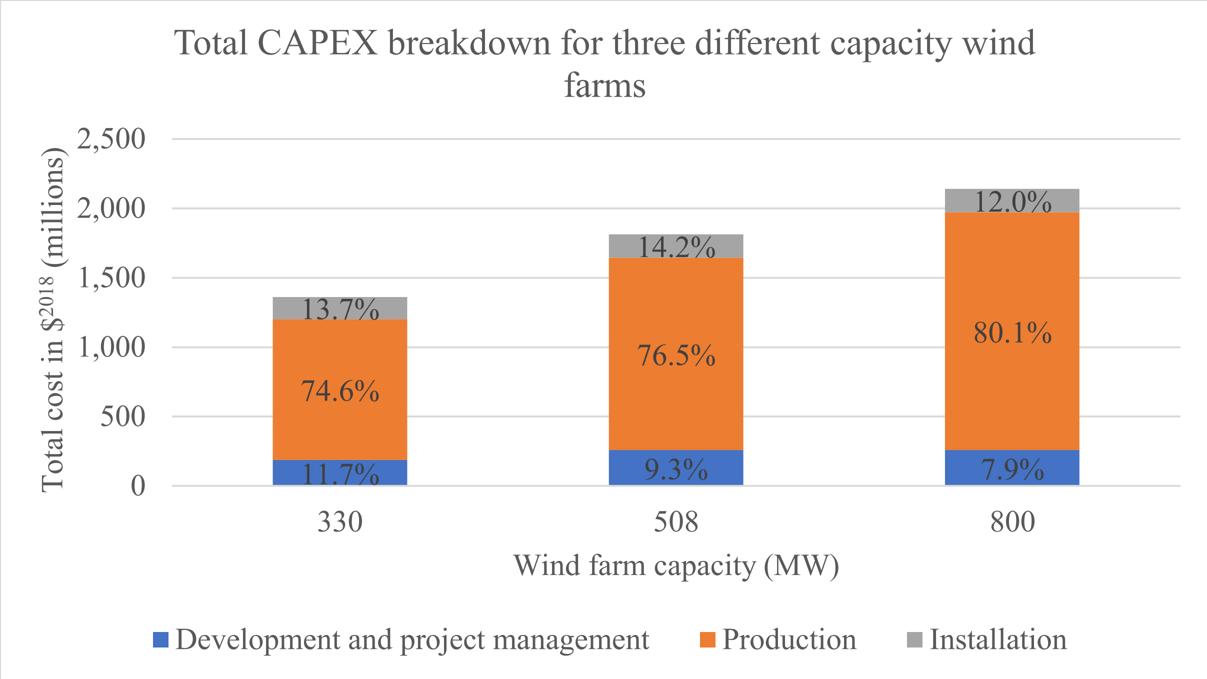

Figure 11 Total CAPEX breakdown for three different capacity wind farms, where 508 MW capacity wind farm is the benchmark case in the present study.

As seen from Figure 11, the total CAPEX cost for the benchmark case is around $^{2018} 1,800 million, where the Production cost occupies the most (around 76.5% of the total CAPEX). It is noted that, by increasing the wind farm capacity, the percentage of production cost is increasing as the turbine size increases significantly. However, the percentage of development and project management cost is decreased. In addition, the percentage of installation cost shows a different trend, where 508 MW wind farm has the largest percentage of installation cost.

5.2. Breakdown of spending during wind farm life cycle

Operational and maintenance expenditure (OPEX) makes up a large portion of lifetime expenditures, however, this cost is spread across the life span of the offshore wind farm. Figure 12 illustrates the cost distributions over the life cycle of the benchmark case. As it can be seen, the majority of the cost occurs before the commissioning year (Year 0 in Figure 12). And the production cost occupies a huge part of it. In addition, the decommissioning cost occupies a relatively small portion of the total life span cost. The O&M cost decreases over the time after the commissioning year.

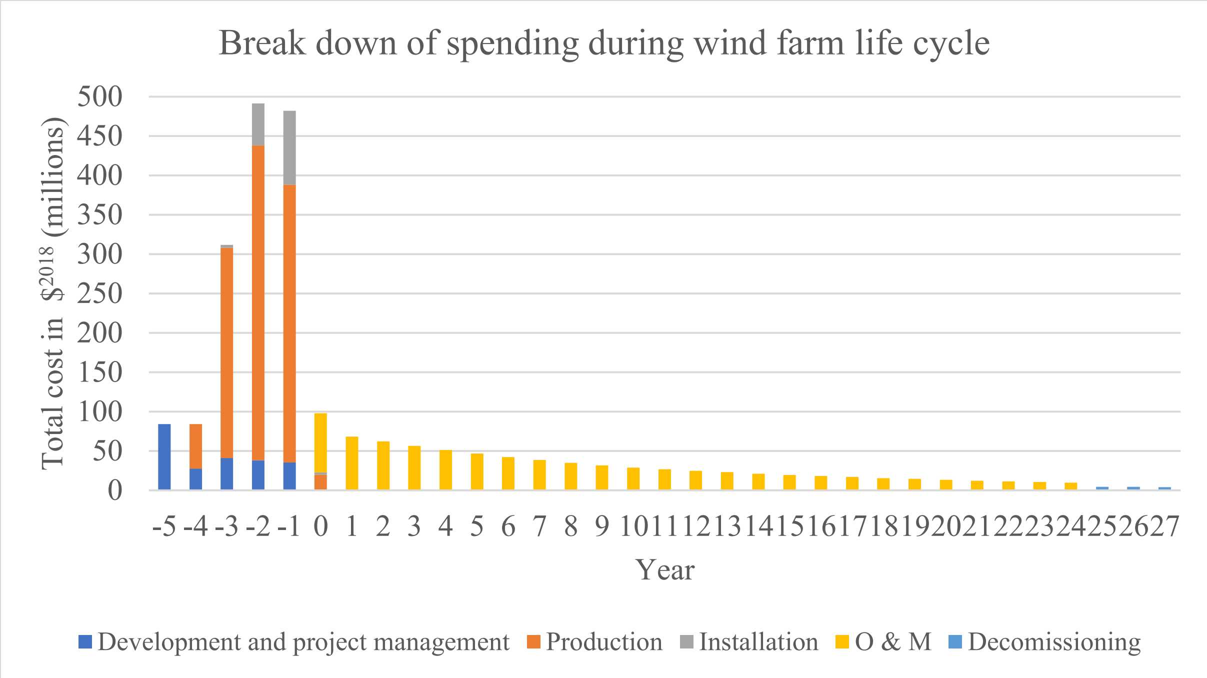

Figure 12 Breakdown of spending during wind farm life cycle (for the benchmark case).

5.3. Power output along with the life span

Figure 13 illustrates the power output throughout the life span of the wind farm. As shown in Figure 13, the power output of larger capacity wind farm declines faster than that of the lower capacity wind farm. At the end of the life span, the power output difference between the three different capacity wind farms is much smaller than when the wind farm is commissioned.

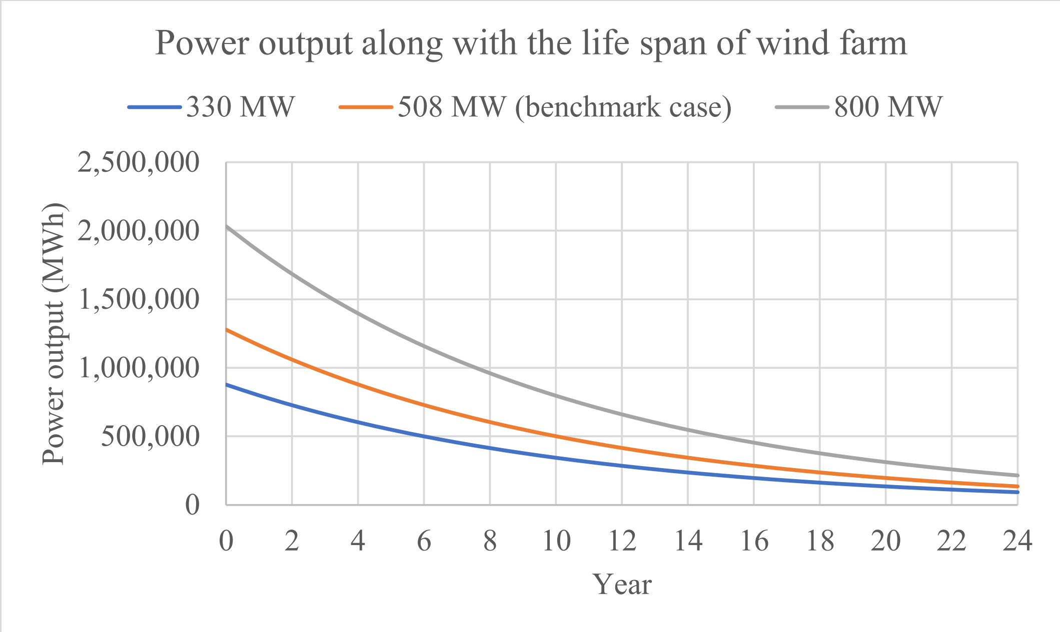

Figure 13 Power output along with life span for three different capacity wind farms (operated at Site B), where 508 MW capacity wind farm is the benchmark case in the present study.

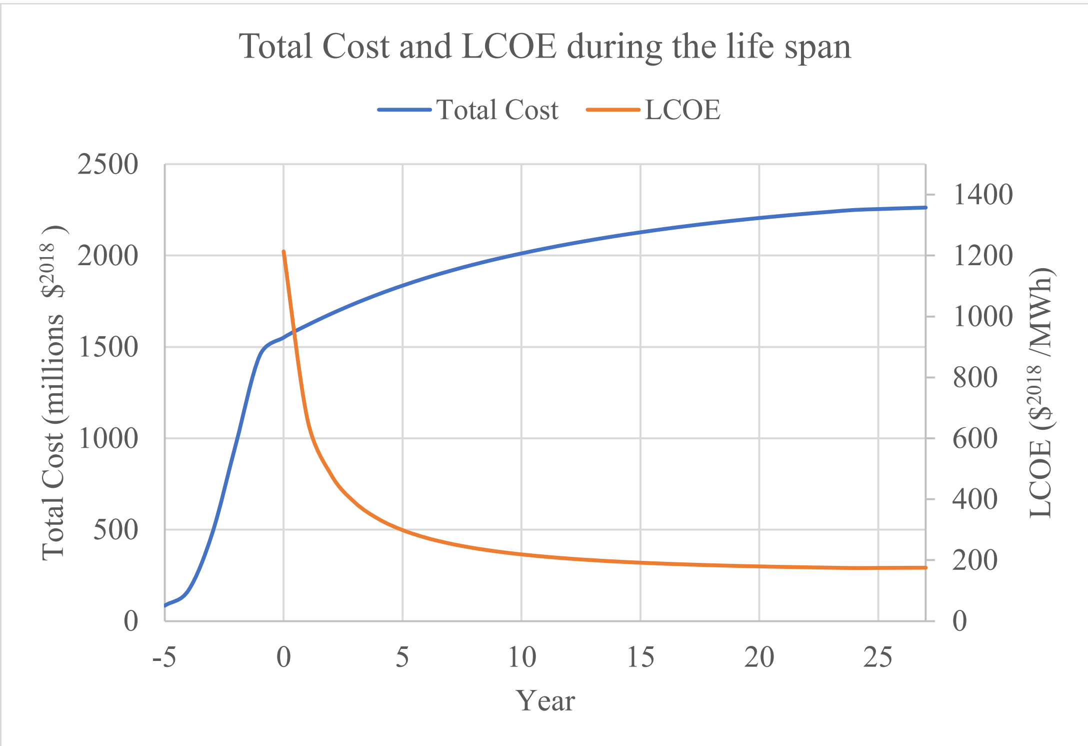

Figure 14 Total Cost and LCOE of the benchmark wind farm during the life span.

As it can be seen in Figure 14, there is a significant increment of total cost spent on the project from the "year -4" to the "year -1", since the majority of the production activities is carried out during these 4 years. After the start of operations from the year "0", the rate of increase of the total cost slows down. Additionally, it is noted that the LCOE is extremely high in the first 5 years from the commissioning year (the "year 0"). This is due to that the CAPEX occupies a huge amount of the total cost at the first few years. At "year 5", the LCOE (298.7 $\$^{2018}$/MWh) is almost two times larger than the LCOE value at "year 27" (175.1 $\$^{2018}$/MWh, the wind farm is fully decommissioned). However, the value of LCOE becomes relatively constant after "year 10" (218.8 $\$^{2018}$/MWh at the "year 10", which is 1.25 times of the final LCOE value). Only 2.5% difference has been observed between the LCOE at year 20 and year 27. If the wind farm is decommissioned at year 19, which means it has a life span of 20 years, the value of LCOE is 182.8 $\$^{2018}$/MWh, 4.4% larger than the benchmark case. Thus, increasing the life span of a wind farm can decrease the expected value of LCOE.

5.4. Sensitivity analysis on the levelised cost of energy

5.4.1. Wind turbine type effect on LCOE

The present LCOE results are evaluated based on the numerical model presented in the methodology section. The results from the benchmark case together with two different rated power turbine wind farms (with same operation site and operation height) are compared in this section, in order to evaluate the effect of the different rated power of wind turbines. Figure 15 presents the breakdown of LCOE cost for the three wind farms. It is clearly shown that the LCOE is decreased by increasing the capability of the wind farm.

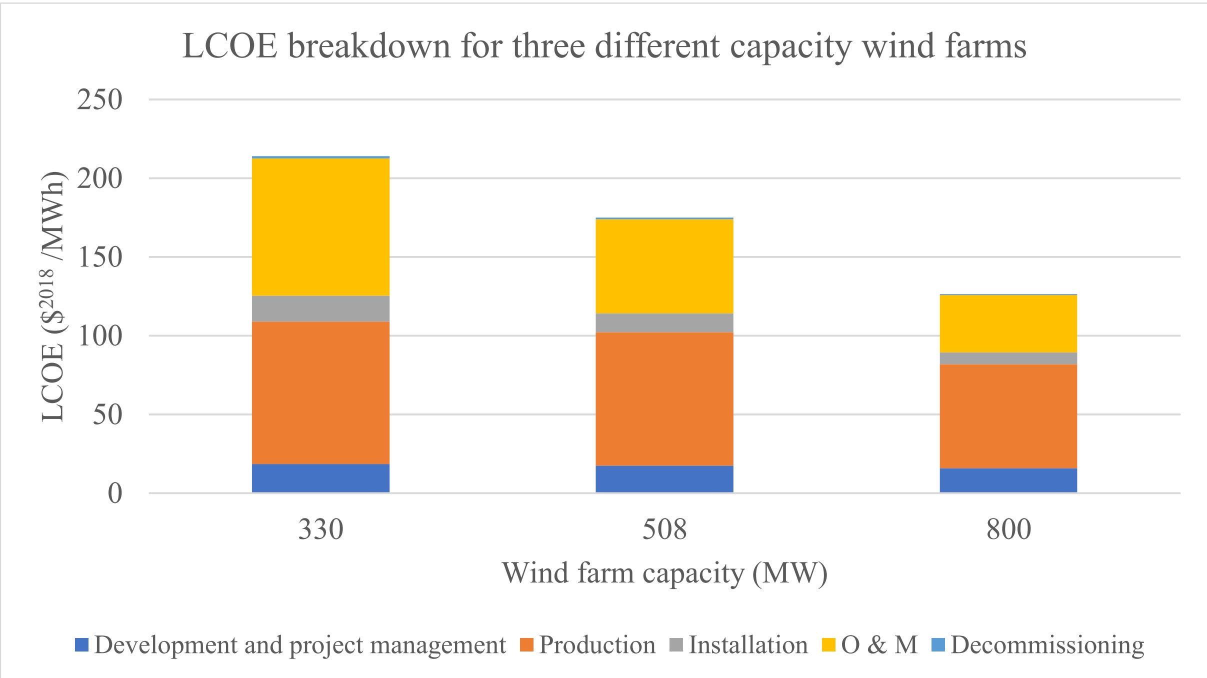

Figure 15 LCOE cost breakdown for three different capacity wind farms (508 MW is the benchmark case).

Additionally, by summarising the present results from LCOE, the minimum and maximum LCOE results (along with the case condition) are illustrated in Table 25.

Table 25 Maximum and Minimum LCOE results in the present study.

Maximum LCOE cost				
Wind turbine Type	**Operation Site**	**Distance to the nearest port (km)**	**Operation height (m)**	**LCOE ($\$^{2018}$/MWh)**
Vestas V112-3.3 MW	C	160	85	279.4
Minimum LCOE cost				
Wind turbine Type	**Operation Site**	**Distance to the nearest port (km)**	**Operation height (m)**	**LCOE ($\$^{2018}$/MWh)**
Vestas V164-8.0 MW	A	32 km	115	123.4

5.4.2. Life span effect on LCOE

As shown in Figure 16, for a short project life span (less than 5 years), the LCOE is extremely high as the energy production cannot cover most of the development cost. However, when the project life span reaches to a certain level (in the present case, more than 20 years), the LCOE is converged around 170 ~ 180 $\$^{2018}$/MWh (182.8 $\$^{2018}$/MWh for a 20-year project life span and 166.3 $\$^{2018}$/MWh for a 50 years life span).

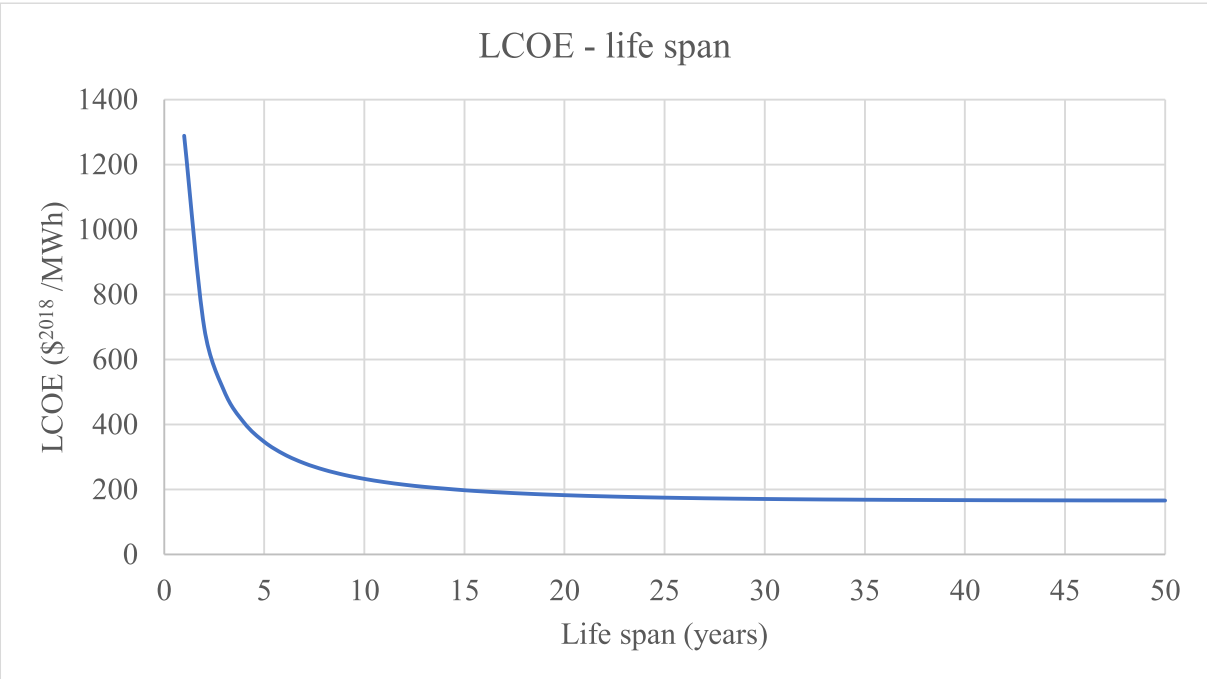

Figure 16 Effect of the project life span on LCOE.

5.4.3. Operation site effect on LCOE

As can be seen in Figure 17, the effect of wind farm capacity shows that the wind farms operated at Site A and Site B have a very similar trend as the capacity increases. However, there is a relatively large decrement of LCOE at Site C when the capacity changes from 330 MW to 508 MW. In addition, in Figure 18, when the wind farm is positioned further away than 70 km (around Site B) to the nearest port, the LCOE increases rapidly compared with the results between 30 km to 70 km.

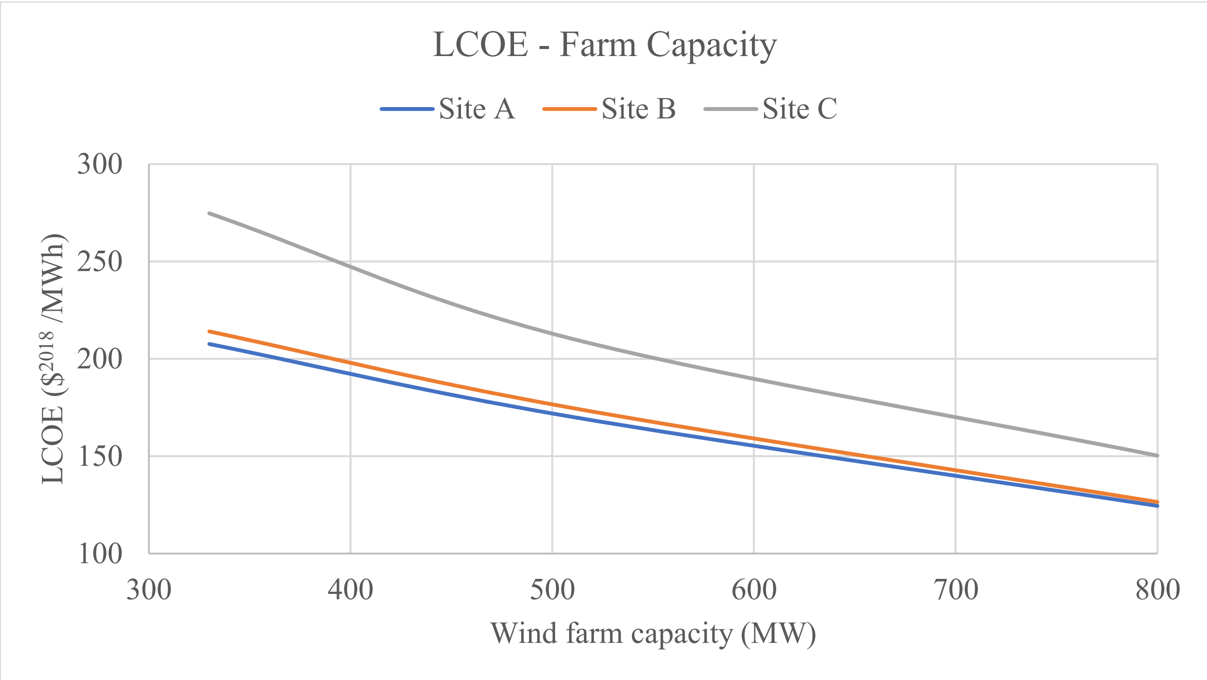

Figure 17 Effect of the farm capacity of operation site on LCOE.

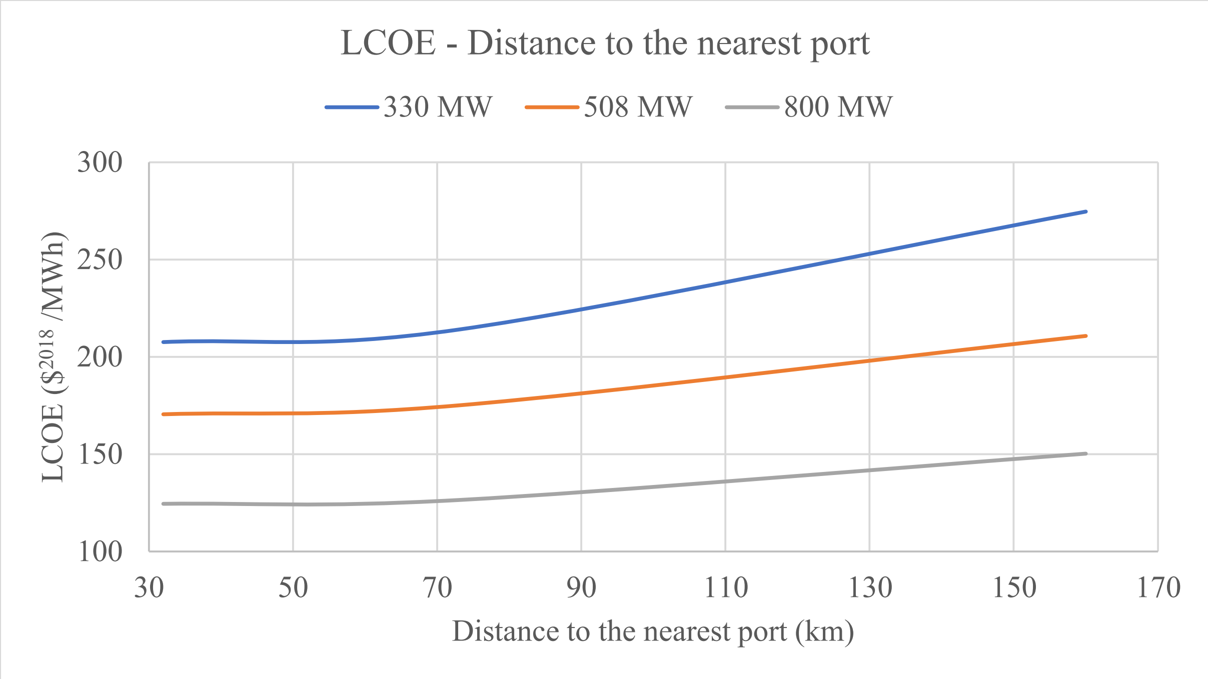

Figure 18 Effect of the distance to the nearest port (operation site location) on LCOE.

5.4.4. Operation height effect on LCOE

In this section, the wind turbine operation height effect on the performance of LCOE is discussed. As can be seen in Figure 19, the effect of operation height is not critical compared with other factors. However, this is based on the assumption that the tower can completely support the wind turbine in a reasonable way. Thus, the operation height range is limited in the present work.

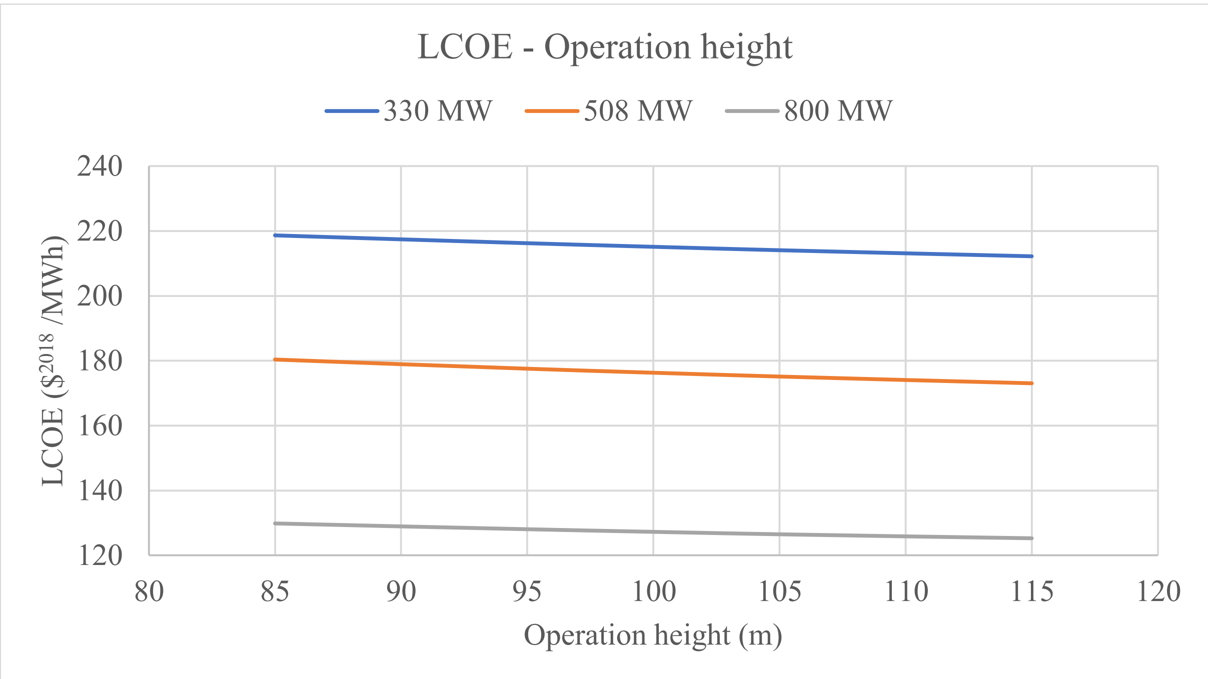

Figure 19 Effect of the wind turbine operation height on LCOE.

5.4.5. Seasonal performance effect on LCOE

The O & M strategy in the current investigation follows an annual plan (Beiter et al., 2016a), however, as it can be seen in Figure 4, Figure 5 and Figure 6, the wind profile varied significantly between Q1, Q4 and Q2, Q3. Thus, it is worth to carry out an investigation to see the O & M plan effect on LCOE. A general assumption is made that all O & M activities are carried out within one specific quarter of a year and the LCOE results based on this assumption are presented in this section. The cases compared are operated at Site C with an operation height of 115 m. In Q1 and Q4, the majority of the wind speeds locate within the range of 10 ~ 15 m/s. However, in Q2 and Q3, most of the wind speeds locate within the range of 5 ~ 10 m/s, which are much lower than Q1 and Q4. Therefore, perform O & M activities in Q1 and Q4 could sacrifice more wind resources when it around rated speed. And the severe metocean condition will bring more cost on the O & M. As the results show (Table 26), when O & M is only performed within Q1 and Q4, the LCOE increased about 3% compared with the yearly basis O & M plan. Thus, a yearly O & M plan is still suggested from the present study.

Table 26 Seasonal O & M plan effect on LCOE results.

			330 MW wind farm		
O & M strategy	**Only in Q1**	**Only in Q2**	**Only in Q3**	**Only in Q4**	**Annual plan**
LCOE ($\$^{2018}$/MWh)	282.8	274.5	275.0	282.7	272.9
			508 MW wind farm		
O & M strategy	**Only in Q1**	**Only in Q2**	**Only in Q3**	**Only in Q4**	**Annual plan**
LCOE ($\$^{2018}$/MWh)	218.1	209.9	210.4	217.5	208.7
			800 MW wind farm		
O & M strategy	**Only in Q1**	**Only in Q2**	**Only in Q3**	**Only in Q4**	**Annual plan**
LCOE ($\$^{2018}$/MWh)	155.3	150.2	150.5	155.1	149.3

5.5. Energy Density

As the land space is limited onshore for a large wind farm, the placement of these enormous wind farms over the ocean has huge advantages. However, for a fix-bottom structure offshore wind farm, the available coastal area is still limited due to the seabed conditions, local government policy and limitations from marine transportation. As the spacing ratio is fixed in the present study, when the wind farm consists of large wind turbines, the occupied area of the wind farm is also increased. The occupied areas (excluding substations) of the wind farms considered in the present study are listed in Table 27 and it can be seen that the occupied coastal area of the 800 MW wind farm is over 2 times the area of the 330 MW wind farm. Based on this, a novel factor named Wind Farm Energy Density (WFED) is provided to assess the wind farm performance against the occupied area. The Wind Farm Energy Density (WFED) is calculated as:

$$WFED = \frac{Total\ Lifetime\ Power\ Output}{Wind\ Farm\ Area} \quad (18)$$

where, the Total Lifetime Power Output is the life span electricity generated by the wind farm (MWh) and the Wind Farm Area is the wind farm occupied coastal area excluding the offshore substation (km^2).

Table 27 Wind farm occupied offshore area.

Wind farm capacity (MW)	**330**	**508**	**800**
Wind farm area (km^2)	49,787,136	63,011,844	106,750,224

Figure 20 and Figure 21 present the wind farm capacity and operation site locations effects on WFED. As can be seen in both figures, the 508 MW wind farm has the best performance among the wind farms investigated. In addition, the WFED results for Site A and Site B are very similar while significantly higher results have been observed at Site C. This is due to the higher wind speed at Site C compared to Sites A and B.

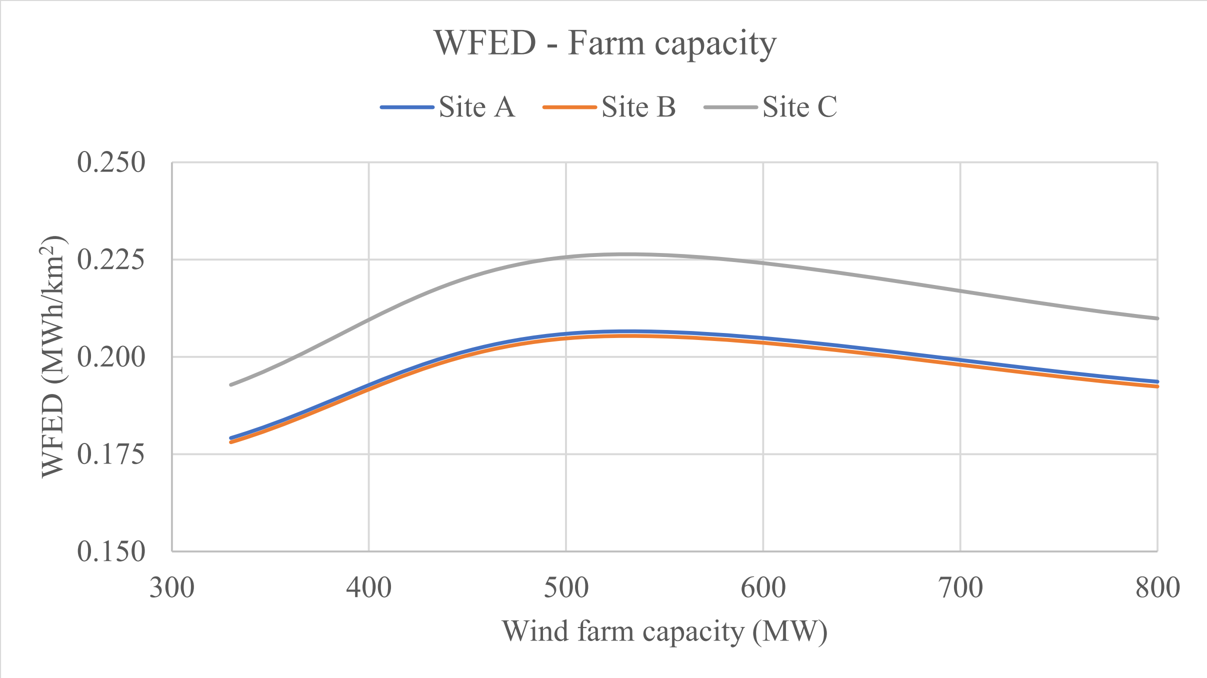

Figure 20 Effect of the farm capacity of operation site on WFED.

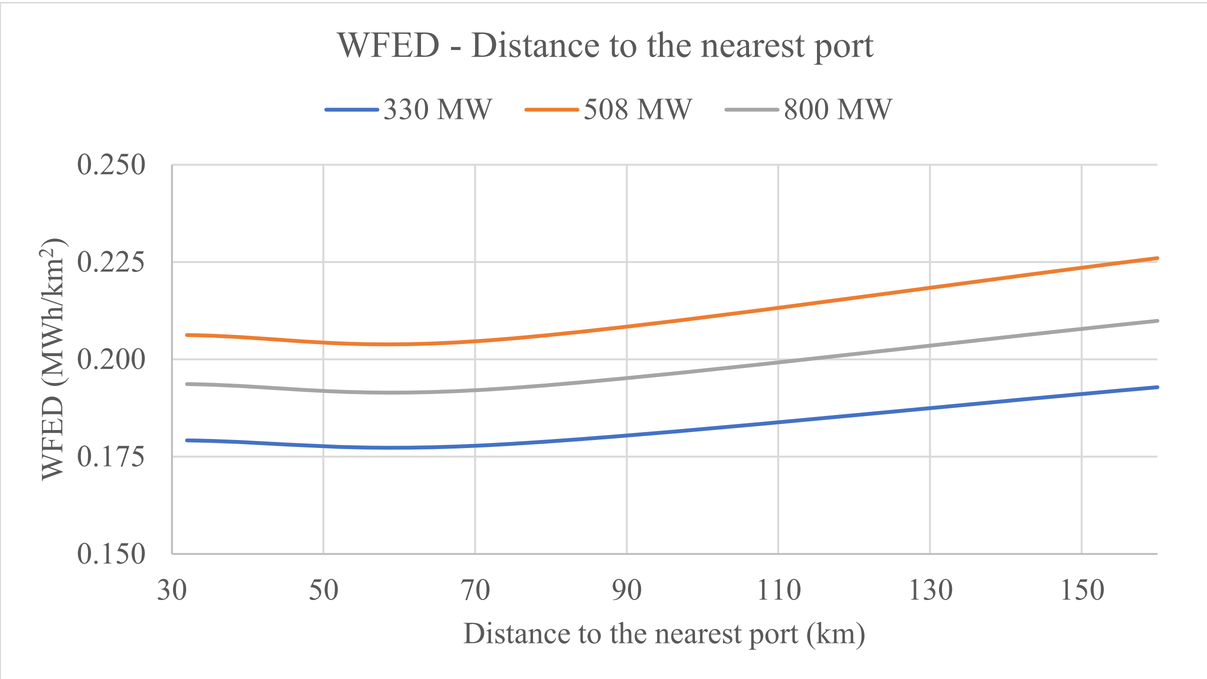

Figure 21 Effect of the distance to the nearest port (operation site location) on WFED.

It is demonstrated that, when considering the limited coastal area as an issue, a large capacity wind farm may not have good performance compared with a smaller wind farm in a way of energy production. However, the larger wind farm still offers lower LCOE results in the present work. The WFED factor will serve as an additional factor for future decision makings.

6. Conclusions

In the present work, a case study of LCOE based on the potential developments at the offshore area of the New York State is provided. A comprehensive numerical model of predicting the LCOE for a fix-bottom concept wind farm is produced based on the available pieces of literature. Some specific local limitations in the United States (e.g. Jones Acts factor) are considered in the current work following in line with the present European development experience. A ten-year historical wind data set is used to evaluate the wind farm energy production. The effects of distance to shore, rated power, life span, turbine operation height, farm capacity and seasonal operation plan on LCOE are evaluated in detail.

The results indicate that the energy from a monopile concept wind farm may produce a value of LCOE reaching to 123.4 $\$^{2018}$/MWh. The optimised conditions (800 MW wind farm operated at Site A with a turbine operation height of 115 m) are identified in the present study. It is noted that by increasing the wind farm capacity (wind turbine rated power), LCOE can be decreased significantly. In addition, the present study indicates that a wind farm operated at a site close to the shore will have a lower LCOE compared with a site operated far from the shore. This is due to the operation and maintenance cost which is mainly driven by the distance from the shore. The effects of operation height are relatively small compared with other factors. The current LCOE study also indicates that with a project life span more than 20 years, the LCOE will not alter significantly. Thus, a more than 20 years life span is suggested for the wind farm development. It is noted that, the present investigation still suggests an annual operation and maintenance plan. If O & M activities are carried out in one specific quarter, it demonstrates that the results of LCOE will be increased compared with yearly basis O & M strategy.

A novel factor for evaluating the wind farm performance over coastal area is suggested and named as wind farm energy density (WFED) in the present work. An analysis of WFED for the different case scenarios showed that when considering the limited coastal area as an issue, a large capacity wind farm may not have a good performance compared with a smaller wind farm based on their energy production. The 508 MW wind farm has a better WFED value compared with either 330 MW wind farm or 800 MW wind farm in all sites.

Further developments on the overall numerical model are being considered in order to expand the current concept to offshore floating wind farm development. In addition, further developments on the lifetime extension and detailed decommissioning study are also suggested by the authors.

Acknowledgement

The authors gratefully acknowledge that the research presented in this paper was partially generated as part of the HORIZON 2020 SHIPLYS (Ship Life Cycle Software Solutions) Project, Grant agreement number 690770.

Reference

2006. 46. U.S.C. § 50101 et seq.

A/S, V.W.S., 2013. OFFSHORE V164-8.0 MW V112-3.3 MW, Hedeager 44 . 8200 Aarhus N . Denmark

AG, R.S., The 5-megawatt power plant with 126 metre rotor diameter, Überseering 10 · 22297 Hamburg · Germany.

AG, R.S., 5M. REpower Systems AG Überseering 10 · 22297 Hamburg · Germany

Agency, I.R.E., 2012. Renewable Energy Technologies: Cost Analysis Series - Wind Power. International Renewable Energy Agency, United Arab Emirates.

Alibaba, 2019a. Prestressed concrete Hangzhou: Alibaba Group.

Alibaba, 2019b. S355 plates, Hangzhou: Alibaba Group.

Allan, G., Gilmartin, M., McGregor, P., Swales, K., 2011. Levelised costs of Wave and Tidal energy in the UK: Cost competitiveness and the importance of “banded” Renewables Obligation Certificates. Energy Policy 39 (1), 23-39.

Ancona, D., McVeigh, J., Wind turbine-materials and manufacturing fact sheet.

Association, E.W.E., 2009. The economics of wind energy. EWEA.

Astariz, S., Vazquez, A., Iglesias, G., 2015. Evaluation and comparison of the levelized cost of tidal, wave, and offshore wind energy. Journal of Renewable and Sustainable Energy 7 (5), 053112.

Authority, N.Y.S.E.R.a.D., 2017. Area for Consideration for the Potential Locating of Offshore Wind Energy Areas, New York State, U.S.

Beiter, P., Musial, W., Smith, A., Kilcher, L., Damiani, R., Maness, M., Sirnivas, S., Stehly, T., Gevorgian, V., Mooney, M., 2016a. A Spatial-Economic Cost Reduction Pathway Analysis for US Offshore Wind Energy Development from 2015–2030. National Renewable Energy Laboratory, September.

Beiter, P., Musial, W., Smith, A., Lantz, E., Kilcher, L., Damiani, R., Maness, M., Sirnivas, S., Stehly, T., Gevorgian, V., 2016b. Estimating the Economic Potential of Offshore Wind in the United States. National Renewable Energy Lab.(NREL), Golden, CO (United States).

Bjerkseter, C., Ågotnes, A., 2013. Levelised costs of energy for offshore floating wind turbine concepts. Norwegian University of Life Sciences, Ås.

Branker, K., Pathak, M., Pearce, J.M., 2011. A review of solar photovoltaic levelized cost of electricity. Renewable and Sustainable Energy Reviews 15 (9), 4470-4482.

Castro-Santos, L., Diaz-Casas, V., 2014. Life-cycle cost analysis of floating offshore wind farms. Renewable Energy 66, 41-48.

Castro-Santos, L., Diaz-Casas, V., 2015. Sensitivity analysis of floating offshore wind farms. Energy Conversion and Management 101, 271-277.

Castro-Santos, L., Filgueira-Vizoso, A., Lamas-Galdo, I., Carral-Couce, L., 2018. Methodology to calculate the installation costs of offshore wind farms located in deep waters. Journal of Cleaner Production 170, 1124-1135.

Center, N.D.B., 2018. National Oceanic and Atmosphercic Adminstration's National Data Buoy Center.

De Vries, W., Vemula, N.K., Passon, P., Fischer, T., Kaufer, D., Matha, D., Schmidt, B., Vorpahl, F., 2011. Final report WP 4.2: support structure concepts for deep water sites: deliverable D4. 2.8 (WP4: offshore foundations and support structures).

EEA, 2017. Renewable energy in Europe 2017. European Environment Agency, Luxembourg: Publications Office of the European Union.

Enterprise, S., 2016. Oil and Gas 'Seize the Opportunity' Guides Offshore Wind. Scottish Enterprise.

The Crown Estate, 2010, A Guide to an Offshore Wind Farm

A Guide to an Offshore Wind Farm, London, UK.

The Crown Estate, 2017. Offshore wind operational report, London, UK.

Faaij, A., Junginger, M., 2004. Cost reduction prospects for the offshore wind energy sector. Utrecht: Utrecht University.

Gonzalez-Rodriguez, A.G., 2017. Review of offshore wind farm cost components. Energy for Sustainable Development 37, 10-19.

Grid, L.N., 2011. Offshore Development Information Statement. .

Guezuraga, B., Zauner, R., Pölz, W., 2012. Life cycle assessment of two different 2 MW class wind turbines. Renewable Energy 37 (1), 37-44.

Hartman, L., 2016. Computing America's Offshore Wind Energy Potential. U.S. Department of Energy, U.S. .

Hegedus, S., Luque, A., 2010. Achievements and challenges of solar electricity from photovoltaics. Handbook of photovoltaic science and engineering, 1-38.

Ioannou, A., Angus, A., Brennan, F., 2018a. A lifecycle techno-economic model of offshore wind energy for different entry and exit instances. Applied Energy 221, 406-424.

Ioannou, A., Angus, A., Brennan, F., 2018b. Parametric CAPEX, OPEX, and LCOE expressions for offshore wind farms based on global deployment parameters. Energy Sources, Part B: Economics, Planning, and Policy 13 (5), 281-290.

Jonkman, J., Butterfield, S., Musial, W., Scott, G., 2009. Definition of a 5-MW reference wind turbine for offshore system development.

Lai, C.S., McCulloch, M.D., 2017. Levelized cost of electricity for solar photovoltaic and electrical energy storage. Applied energy 190, 191-203.

Lerch, M., De-Prada-Gil, M., Molins, C., Benveniste, G., 2018. Sensitivity analysis on the levelized cost of energy for floating offshore wind farms. Sustainable Energy Technologies and Assessments 30, 77-90.

Logan, B.V.G.H.K.F.A.R.A., 2017. Future renewable energy costs: Offshore wind. BVG Associates; InnoEnergy, InnoEnergy.

Lubitz, W.D., 2014. Impact of ambient turbulence on performance of a small wind turbine. Renewable Energy 61, 69-73.

Maienza, C., Avossa, A., Ricciardelli, F., Coiro, D., Troise, G., Georgakis, C.T., 2020. A life cycle cost model for floating offshore wind farms. Applied Energy 266, 114716.

Mattar, C., Guzmán-Ibarra, M.C., 2017. A techno-economic assessment of offshore wind energy in Chile. Energy 133, 191-205.

May, T.W., Yeap, Y.M., Ukil, A., 2016. Comparative evaluation of power loss in HVAC and HVDC transmission systems, Region 10 Conference (TENCON), 2016 IEEE. IEEE, pp. 637-641.

Meinshausen, M., Meinshausen, N., Hare, W., Raper, S.C., Frieler, K., Knutti, R., Frame, D.J., Allen, M.R., 2009. Greenhouse-gas emission targets for limiting global warming to 2 C. Nature 458 (7242), 1158.

Myhr, A., Bjerkseter, C., Ågotnes, A., Nygaard, T.A., 2014. Levelised cost of energy for offshore floating wind turbines in a life cycle perspective. Renewable Energy 66, 714-728.

NOAA/OER, 2002. General bathymetry of the coastal ocean in the New York-New Jersey metropolitan region., Detailed bathymetric data provides a framework for future exploration.

Obi, M., Jensen, S., Ferris, J.B., Bass, R.B., 2017. Calculation of levelized costs of electricity for various electrical energy storage systems. Renewable and Sustainable Energy Reviews 67, 908-920.

OpenEI, 2019. Transparent Cost Database.

P.(PVC), 2012. Offshore wind cost reduction pathways study. In: Finanace work stream. The Crown Estate, Longdon, UK.

Pfenninger, S., Keirstead, J., 2015. Renewables, nuclear, or fossil fuels? Scenarios for Great Britain's power system considering costs, emissions and energy security. Applied energy 152, 83-93.

Short, W., Packey, D.J., Holt, T., 1995. A manual for the economic evaluation of energy efficiency and renewable energy technologies. National Renewable Energy Lab., Golden, CO (United States).

Staffell, I., Green, R., 2014. How does wind farm performance decline with age? Renewable Energy 66, 775-786.

Tremeac, B., Meunier, F., 2009. Life cycle analysis of 4.5 MW and 250 W wind turbines. Renewable and Sustainable Energy Reviews 13 (8), 2104-2110.

Veatch, B., 2010. Levelized Cost of Energy Calculation, Overland Park: Black & Veatch.

Voormolen, J., Junginger, H., Van Sark, W., 2016. Unravelling historical cost developments of offshore wind energy in Europe. Energy Policy 88, 435-444.

Wagner, R., Courtney, M., Larsen, T.J., Paulsen, U.S., 2010. Simulation of shear and turbulence impact on wind turbine performance.

Wiser, R., Hand, M., Seel, J., Paulos, B., 2016. Reducing Wind Energy Costs through Increased Turbine Size: Is the Sky the Limit? Lawrence Berkeley National Laboratory.